Zeitschrift: Helvetica Physica Acta
Band: 46 (1973)
Heft: 1

Artikel: Gamma decay properties of 3^- levels in even-even nuclei
Autor: Roehmer, F.C.
DOI: https://doi.org/10.5169/seals-114472

Helvetica Physica Acta
Vol. 46, 1973.
Birkhäuser Verlag Basel

Gamma Decay Properties of 3^- Levels in Even–Even Nuclei

by **F. C. Roehmer**

Laboratory for High Energy Physics, Swiss Federal Institute of Technology, Zurich,
c/o Swiss Institute for Nuclear Research, CH-5234 Villigen, Switzerland

(11. IX. 72)

Summary. The gamma decay characteristics of 3^- states in ^{38}Ar, ^{140}Ce and ^{160}Dy have been investigated using radioactive sources. The discrepancy between conflicting energy values reported for the gamma rays depopulating the 3^- level in ^{38}Ar has been removed, and this state was shown to lie at 3808 ± 2 keV. The $E3$ groundstate transition has been observed and an enhancement factor of 17 ± 4 relative to the single particle unit (s.p.u.) has been deduced. From gamma–gamma angular correlation measurements on the 867.8–1596.6 keV cascade we determined the spin and parity of the 2464.4 keV level in ^{140}Ce to be 3^-. The groundstate transition from this state was discovered and an intensity limit for the $3^- \rightarrow 4_1^+$ transition was obtained. From these data follows: the $3^- \rightarrow 2_1^+$ transition is the fastest one of this type with $B(E1) = (3.1 \pm 0.5) \cdot 10^{-3}$ s.p.u.; the $3^- \rightarrow 4_1^+$ transition has $B(E1) < 5.5 \cdot 10^{-5}$ s.p.u.; the ratio $B(E1, 3^- \rightarrow 4_1^+)/B(E1, 3^- \rightarrow 2_1^+) < 1.6 \cdot 10^{-2}$ is the smallest one yet known. The 1286 keV transition in ^{160}Dy, which formerly was tentatively interpreted as the groundstate transition from the 3_1^- level at 1286.7 keV, was proven to originate not from this level. An intensity limit for the groundstate transition from the 3_2^- state at 1399.0 keV has been determined.

A compilation of some properties of the lowest 3^- states of even–even nuclei is presented. The excitation energies show pronounced shell effects (maxima at $N = 28$, 50, 82, 126 and $Z = 28$, 50, 82); the excitation probabilities $B(E3)$ are not positively related to the magic numbers. The largest $B(E1, 3^- \rightarrow 2_1^+)$ values are observed at $N = 20$ and 82, but the data are too scarce to recognize any regularity.

Together with the angular correlation of the 867.8–1596.6 keV gamma cascade in ^{140}Ce, we also measured those of five transitions in the energy region of 750–950 keV and determined their mixing ratios. The spin and parity assignments for the corresponding levels were confirmed.

1. Introduction

A large number of 3^- collective octupole states has been observed in even–even nuclei throughout the periodic system. The properties of these levels which suggest a collective description are

a) The excitation probabilities are greatly enhanced relative to the single particle estimate.
b) The systematic occurrence of the 3^- states in almost all even–even nuclei suggests that they are due to an excitation of the nucleus as a whole rather than to a specific nucleon.
c) The log ft values observed for allowed transitions to the 3^- levels are systematically high and indicate a structure very different from that of the groundstate of the odd–odd parent nucleus.

Soon after the earliest treatments of collective vibrations, it was recognized that the shell structure has a strong effect on the collective properties of the individual nuclei. The first step in the direction of combining collective and particle aspects of the nucleus was the unified model introduced by Bohr and Mottelson [1] who shifted the emphasis from the collective motion of the particles to the collective motion of the independent-particle field. Since then many calculations were done in order to describe the properties of 3^- levels.

The experimental information which is necessary to test the predictions of the different calculations is partly rather scarce. Best known are the excitation energies of the 3^- levels, and less well the $E3$ transition probabilities. Very little is known about the transition probabilities of $E1$ transitions depopulating the 3^- states.

The present measurements were undertaken to determine $E1/E3$ gamma ray branching ratios of 3^- levels in ^{38}Ar, ^{140}Ce and ^{160}Dy. These quantities allow one to calculate the transition probabilities if the life-time of the state or the excitation probability $B(E3)$ is known. The nuclei under investigation were selected for practical reasons because their 3^- levels are populated rather strongly in the beta decay of the parent isotopes. In Section 2 we briefly review the experimental techniques which are commonly applied in order to measure the properties of 3^- states. Section 3 is devoted to the description of our experiments and a discussion of the individual results. A more general discussion is attempted in Section 4 where we present a compilation of energies, excitation probabilities and $B(E1, 3^- \rightarrow 2_1^+)$ values of the lowest 3^- levels in even–even nuclei. In the appendix we describe our peak fitting procedure.

2. Experimental Methods Frequently Used to Study 3^- Levels

3^- states can be excited by numerous processes such as Coulomb excitation, electron scattering, inelastic scattering of nuclear particles, nuclear reactions or radioactive decay. Due to limitations in the experimental facilities and/or the theoretical understanding, each of these methods is generally suited for the measurement of only a few specific nuclear properties. In the following we briefly summarize the information which can be obtained by various experimental techniques.

i) Coulomb excitation. This very powerful method is especially well suited for the study of 3^- levels because it supplies a lot of information about the excited states. Provided the energy of the projectiles is so low that the Coulomb field prevents the particles from penetrating into the nucleus the excitation process can be studied without interference from the more complicated nuclear interactions and the matrix elements appearing in the cross-section are the same as those responsible for the emission of gamma radiation.

The relative gamma ray yield, as a function of particle energy, being dependent on the multipole order and the excitation energy may be used to determine these quantities. Due to the fact that an $E3$ transition has a yield function quite different from that of an $E1$ or $E2$ transition it is rather easy to recognize this multipole order. An alternative method for determining the multipole order of the excitation is the comparison of the yield for different bombarding particles. Measurement of the gamma ray angular distribution provides information about the multipole order of the excitation and the decay as well as the spin and parity of the states involved. The angular distribution of the inelastically scattered particles allows the determination of the multipole order of excitation. An important property of 3^- states, the excitation

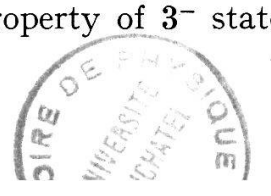

probability, may be obtained also from Coulomb excitation by measuring the absolute cross-section.

For an excellent theoretical and experimental review we refer to a paper by Alder et al. [2].

The transition probability $T(EL)\downarrow$ for an electric transition of multipole order L and energy E from the initial level with spin J_i to the final level with J_f and the reduced transition probability $B(EL)\downarrow$ are related by the expression [3]

$$T(EL)\downarrow = \frac{8\pi(L+1)}{L[(2L+1)!!]^2}\frac{1}{\hbar}\left(\frac{E}{\hbar c}\right)^{2L+1} B(EL)\downarrow.$$

The downward arrows indicate the de-excitation probability. $B(EL)\downarrow$ and $B(EL)\uparrow$ are connected by the relation

$$B(EL)\uparrow = \frac{2J_i+1}{2J_f+1} B(EL)\downarrow.$$

In a simplified single particle model one assumes a central potential without spin-orbit coupling and radial wavefunctions which are constant over the entire nucleus (radius R). If the statistical factor, arising from the integration over the angular wavefunctions, is set equal to one, we obtain the single particle reduced transition probability [3]

$$B_{\text{s.p.}}(EL)\downarrow = \frac{e^2}{4\pi}\left(\frac{3}{3+L}\right)^2 R^{2L}.$$

Since $T(EL)$ is measured in units sec^{-1} and $B(EL)$ very often in $e^2 b^L$ it is convenient to connect both quantities using the numerical values $\hbar c = 19.73$ MeV $b^{1/2}$ and $e^2 = 0.1440$ MeV $b^{1/2}$. With $R = 1.2A^{1/3}$ fm and E in MeV one obtains

$$T(EL)\downarrow = 5.50\cdot 10^{21}\,\frac{L+1}{L[(2L+1)!!]^2}\left(\frac{E}{19.73}\right)^{2L+1} B(EL)\downarrow.$$

ii) *Electron scattering.* The excitation of nuclei by means of electrons has the advantage over Coulomb excitation by nuclear particles in that the interaction is electromagnetic no matter how high the energy of the bombarding particles. The differential cross-section for inelastic scattering as a function of the momentum transfer q is expressed as the square of a form factor $F^2(q)$. From the q dependence of F^2 the multipole order is deduced and extrapolation to $q = 0$ yields the excitation probability.

For details concerning the experiment and its evaluation we refer to the review by Barber [4].

iii) *Nuclear reactions.* Here we deal only with those reactions which may be used to measure the life-time of an excited state by means of the Doppler shift attenuation method. The high energy resolution obtainable in gamma ray measurements with Ge(Li) detectors has greatly improved this method and made it particularly suitable for 3^- levels in lighter nuclei ($A \lesssim 70$), whose life-times generally are of the order of 10^{-13} to 10^{-12} sec.

The most straightforward application of the Doppler shift attenuation method is to use a nuclear reaction that produces recoiling ions which approximate closely a

unidirectional monoenergetic beam. The two types of reactions used nowadays are (particle, gamma) reactions such as (p,γ) and endothermic reactions near the threshold such as $(\alpha,p\gamma)$. The gamma rays emitted during the slowing-down time of the nucleus in a solid or gaseous medium are measured and from the line shape of the observed peak one can deduce the life-time of the excited state.

In general, with the use of a reaction of the type $X(a,b\gamma)\,Y$, the angular distribution of the reaction produces a distribution of recoil directions and energies. In this case one may use a coincidence condition on b to select a unidirectional, monoenergetic beam of recoiling ions which, however, causes low counting rates.

A review of methods for nuclear life-time measurements has been given by Schwarzschild et al. [5].

iv) Inelastic scattering of nuclear particles. In these kind of experiments the nucleus is excited by means of strongly interacting particles. From the analysis of the angular distribution of the scattered particles one obtains the multipole order of the excitation and the deformation parameter of the excited state. The latter quantity is related to the excitation probability, but in a model-dependent way. We refer to a forthcoming paper [6] where we compare reduced transition probabilities $B(E3)$ obtained from electromagnetic measurements with those deduced from deformation parameters.

v) Radioactive decay. Finally, we recall the possibility of exciting a 3^- state by radioactive decay. With modern spectroscopic techniques using Ge(Li) detectors, the energies and branching ratios of depopulating gamma rays can be measured with high accuracy. The latter can be combined with the life-time of the level to calculate transition probabilities. Moreover, conversion electron studies and gamma–gamma angular correlation measurements allow the determination of the multipole order and mode as well as mixing ratios of the de-exciting gamma rays.

From this short survey it is obvious that there exist a variety of experimental methods to study the properties of 3^- levels such as energy, excitation probability and transition probabilities of depopulating gamma rays. As a consequence, the amount of experimental information has increased rapidly in the last years and in many cases the data obtained with different methods provide a check of the reliability of the results.

3. Measurements

3.1. The nucleus ^{38}Ar

The spin and parity assignment of 3^- to the 3808 keV level in ^{38}Ar has been widely accepted based on the results of beta ray spectroscopy and gamma–gamma angular correlation measurements [7]. Robinson [8] observed a weak high-energy gamma ray in the decay $^{38}\mathrm{Cl} \rightarrow {}^{38}\mathrm{Ar}$ which he interpreted as the $E3$ crossover transition from the 3^- level to the groundstate; his energy, however, was smaller than other level energy values [9, 10] by at least 52 ± 12 keV. The present investigation was undertaken in order to resolve this discrepancy and to obtain more accurate energy and intensity determinations. A summary of the results has been reported at the spring meeting of the Swiss Physical Society, 1967 [11].

3.1.1. Measurements and results. The measurements were carried out with a planar Ge(Li) detector of 2.3 ± 0.1 cm^2 area and 4 mm depletion depth coupled to a low noise charge sensitive preamplifier (Tennelec 100C). Further amplification and analysis of

the pulses were performed by an Intertechnique 400-channel analyser system. The efficiency calibration of the detector has been described elsewhere [12]. The ^{38}Cl sources were produced by neutron activation of polychloroethylene $(—CH_2—CCl_2—)_n$ at the reactor SAPHIR of the EIR in Würenlingen, Switzerland. After irradiation of 1 hour the average activity was approximately 1 mCi.

Beginning 5 min after the activation the gamma spectrum was recorded in four periods of 15 min each and the data were stored on magnetic tape. The source to detector distance was typically 8.5 cm; an absorber of 2.5 cm lucite was used to absorb

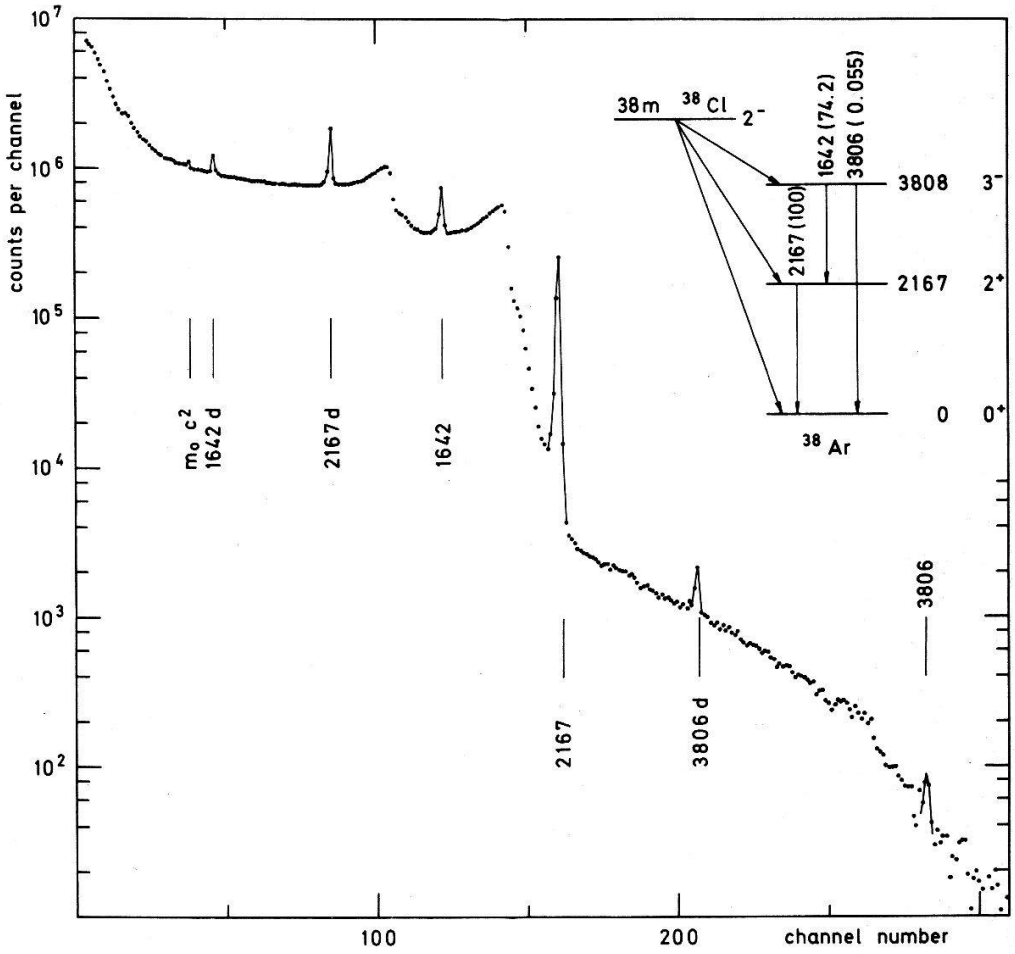

Figure 1
Typical gamma ray spectrum and decay scheme of ^{38}Cl. Energies are in keV. d: double-escape peak.

the beta radiation. For the energy determination we regularly made calibration measurements with ^{60}Co, ^{88}Y and the $^{12}C(n,\gamma)^{13}C$ reaction. The energy values were taken from refs. [13–15]. The energies of the two lower energy gamma rays in ^{38}Ar have been determined in a separate run with an expanded energy scale.

Prior to analysis all spectra were summed (Fig. 1); electronic drifts were compensated before summing by shifting the whole spectrum by an integer number of channels (max. ± 1). In order to determine the peak positions we plotted the count rate in logarithmic scale against the channel number and approximated graphically the slopes of each peak by two straight lines, the intersection of which defined the peak position. Within the errors, no energy non-linearity was observed. For the energy determination we used both full-energy and double-escape peaks.

The count rate under the peaks was determined by totalling the counts channel by channel and subtracting the background under the peak. The uncertainty in the graphic evaluation of the background has been included in the errors. The relative gamma ray intensities deduced from both full-energy and double-escape peaks were in good agreement. All gamma rays followed the half-life of ^{38}Cl [7] and therefore could be assigned to the decay of this isotope.

The results of our energy and intensity measurements are listed in Table 1. The relative intensity of the 3806 keV crossover transition was corrected for the summing of cascade gamma rays in the detector; the pile-up for this line was negligible (<1%). Since the single-escape peak of the 2167 keV transition and the full-energy peak of the 1642 keV line could not be resolved with our detector the intensity of the latter gamma ray was corrected for this contribution.

Table 1

Gamma ray energies and intensities in the decay ^{38}Cl → ^{38}Ar

Energy [keV]	Intensity
1642 ± 2	74.2 ± 3.0
2167 ± 2	100 ± 3.2
3806 ± 3	0.055 ± 0.007

The intensity limits of other gamma rays than those listed in Table 1 are given eslewhere [11].

3.1.2. Discussion. Our gamma ray energies strongly support the position of the 3^- level in ^{38}Ar at 3808 ± 2 keV and eliminate the contradicting energy values reported by Robinson [8]. The results of the present investigation have been incorporated into a consistent decay scheme of ^{38}Cl (Fig. 1) which was confirmed later by van Klinken et al. [16].

It is interesting to look at the decay characteristics of the 3^- level. This state is depopulated by an intense pure $E1$ radiation with $\delta = -0.01 \pm 0.02$ [17] to the first excited 2^+ level and a weak $E3$ transition to the groundstate. From our measurements we deduce a branching ratio $I(E3)/I(E1) = (7.43 \pm 1.00) \cdot 10^{-4}$ which is 6670 ± 890 times larger than according to the single-particle estimate. The life-time of the 3^- state has been measured by Lieb et al. [18] and Engelbertink et al. [19, 20]. Using the average value of 73 ± 16 ps we calculate from our branching ratio that the $E3$ transition is 17.2 ± 4.3 times enhanced relative to the Weisskopf estimate, a value which is well within the region of observed enhancement factors in other nuclei (see Section 4). The $E1$ transition is rather weakly hindered by a factor of 388 ± 83, one of the smallest values yet observed (see Section 4).

3.2. The nucleus ^{140}Ce

The 3^- octupole vibrational state in ^{140}Ce was proposed at 2.47 MeV by Hansen et al. [21] who detected a 0.87 MeV gamma ray in the reaction ^{140}Ce$(\alpha, \alpha' \gamma)^{140}$Ce, which they interpreted as the transition to the first 2^+ state at 1.60 MeV. Even though this level should be populated from the 3^- groundstate of ^{140}La a level at this energy did not appear before the recent work of Baer et al. [22] in previously proposed decay

schemes of ^{140}La. The only evidence for assigning $J^\pi = 3^-$ to this level was the identification of the intense 867.8 keV $E1$ transition with the 0.87 MeV gamma ray reported by Hansen et al. [21]. We therefore decided to measure the angular correlation of the 867.8–1596.6 keV gamma ray cascade (see Fig. 2 for the decay scheme of ^{140}La) to prove the spin assignment of the 2464.4 keV level. We further measured the intensity of the previously unknown $E3$ groundstate transition and looked for the possible

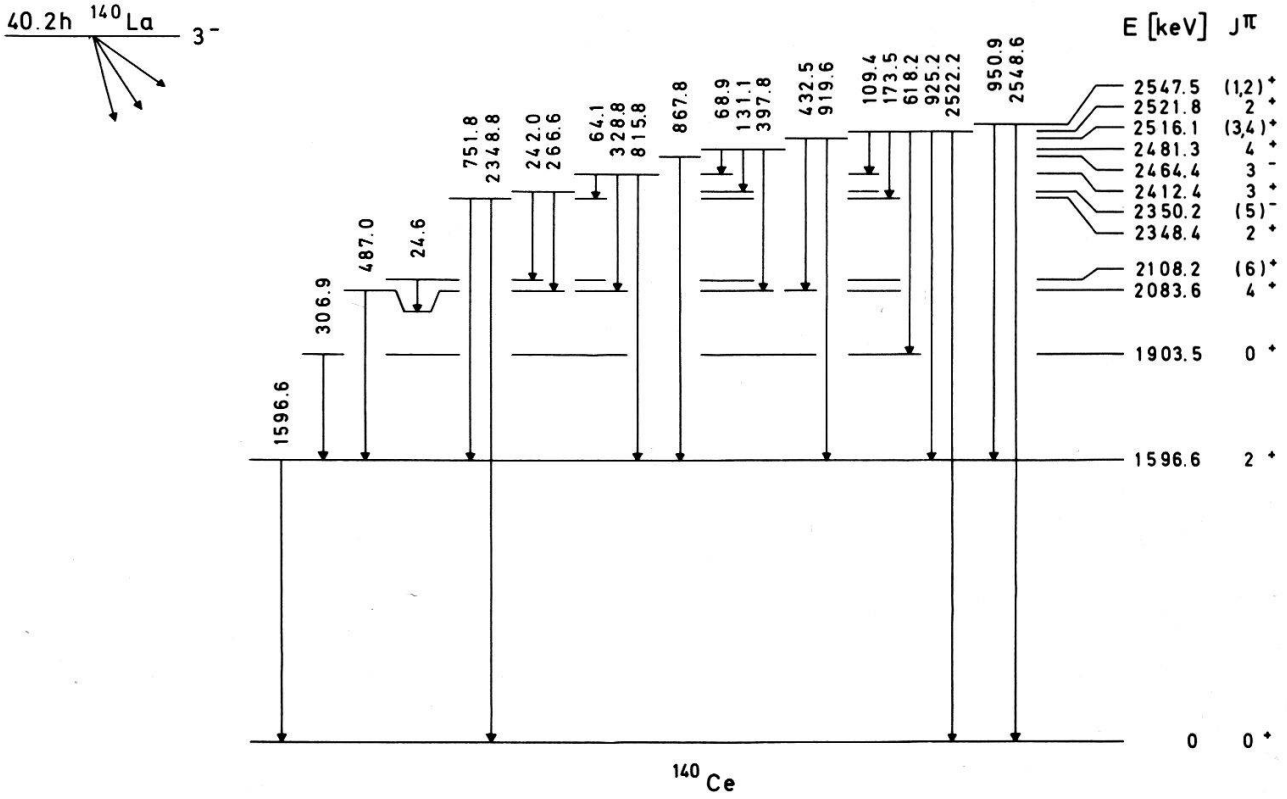

Figure 2
Decay scheme of ^{140}La as proposed by Baer et al. [22]. The excitation energy is not drawn to scale and levels above 3 MeV have been omitted.

$3^- \rightarrow 4^+$ transition. Preliminary results have been reported at meetings of the Swiss Physical Society [23, 24].

3.2.1. Angular correlation measurements

3.2.1.1. Measurements and results. For the anisotropy measurements we used a 40 cm^3 true coaxial Ge(Li) detector (Nuclear Enterprises GD 602) as a fixed detector and a 3″ × 3″ NaI(Tl) detector as movable counter. The block diagram of the fast–slow coincidence circuit (resolving time $2\tau \approx 70$ ns) and the associated electronic equipment is shown in Figure 3. The sources were produced by neutron activation of 99.999% La_2O_3[1]) at the reactor DIORIT of the EIR in Würenlingen, Switzerland. After an irradiation of about 15 min the material was mixed with hydrochloric acid and an activity of about 20 μCi was sealed in a lucite housing. The geometrical details of the source and both detectors are displayed in Figure 4.

[1]) Procured from Koch-Light Laboratories Ltd., Poyle, Colnbrook, Buckinghamshire, England.

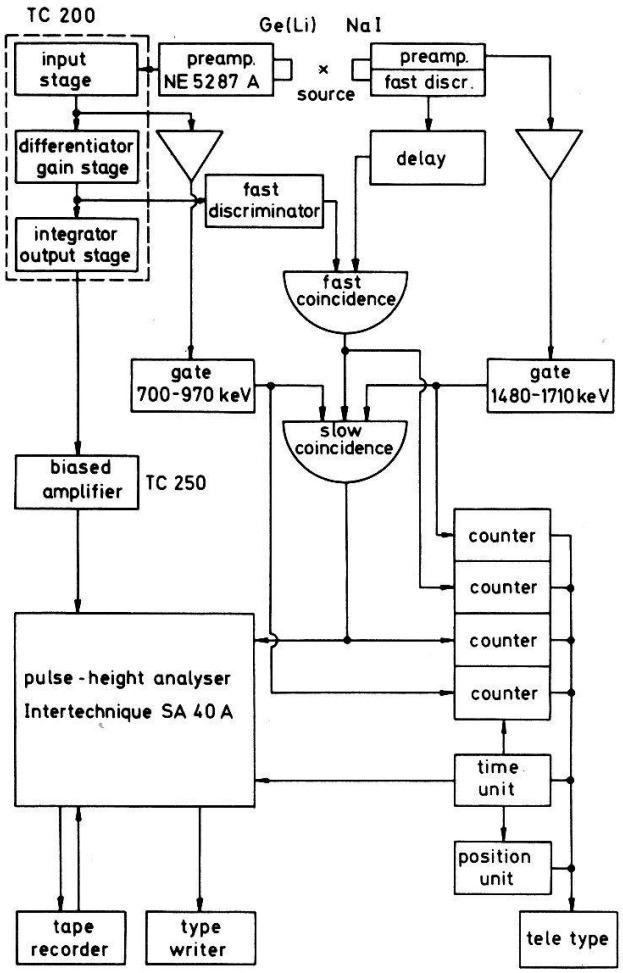

Figure 3
Block diagram of the electronics used for the angular correlation measurements.

The Ge(Li) spectrum in the energy region of 700–970 keV was measured in periods of 10 min in coincidence with the 1596.6 keV transition, alternatively at 90° and 180°. After every five pairs of total coincidence spectra the accidental coincidences were measured which were always less than 20% of the total coincidences.

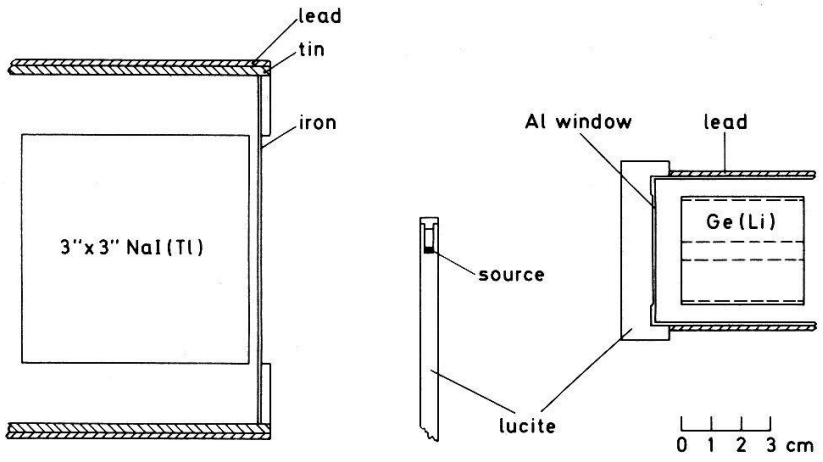

Figure 4
Geometry of the source and both detectors in the angular correlation experiment.

After summing the spectra of total coincidences in groups of five we normalized them by the count rate in the window of the NaI detector and subtracted the normalized accidental coincidences, corrected for the decay of the source. We finally averaged all spectra measured under the same angle channel per channel with the inverse square of the statistical errors as weights to obtain the two spectra of true normalized coincidences, an example of which is displayed in Figure 5.

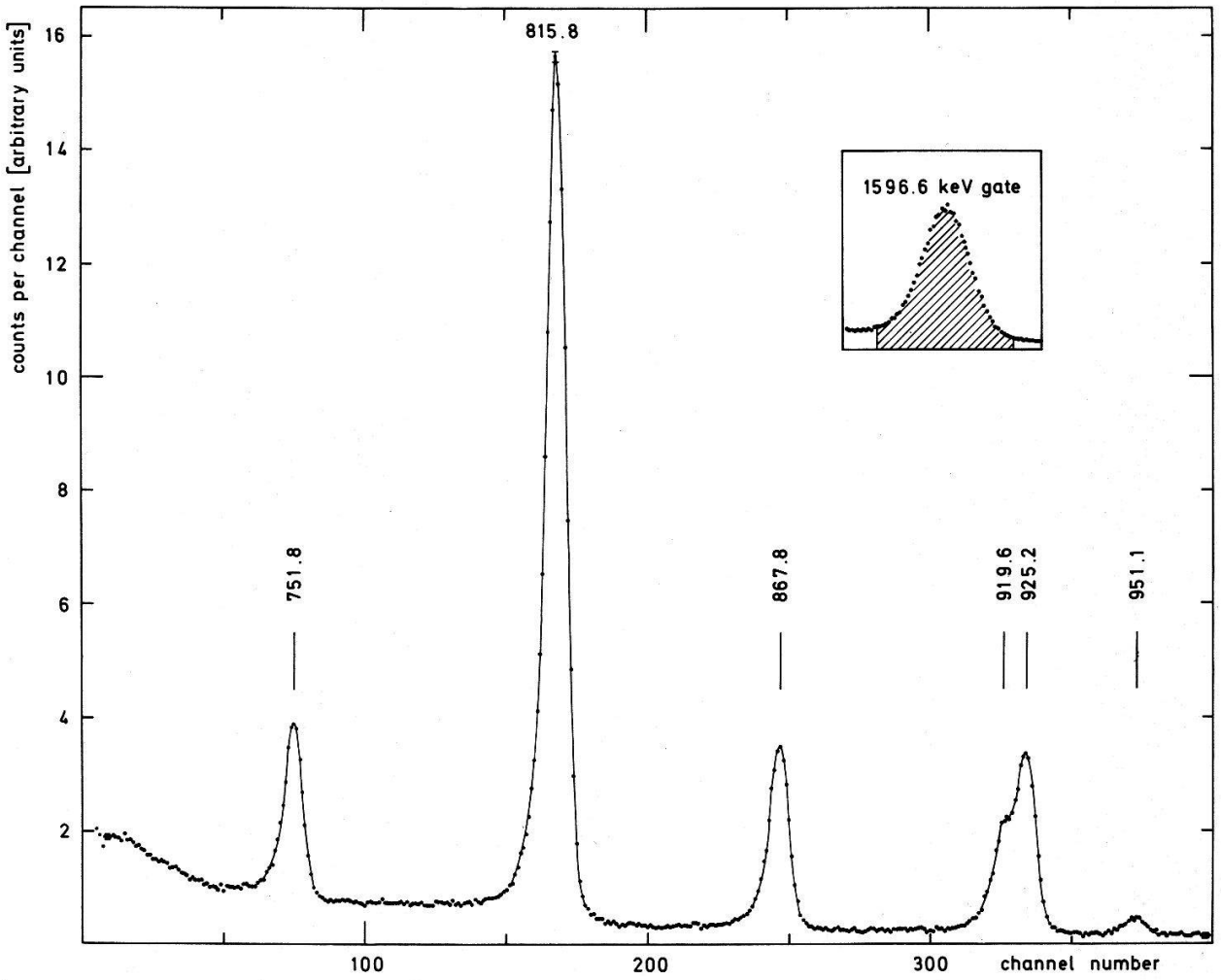

Figure 5
Gamma ray spectrum of ^{140}Ce in the energy region 700–970 keV measured in coincidence with the 1596.6 keV transition under the angle of 90°. Energies are in keV.

The count rates under the peaks were determined by fitting a modified Gaussian (see appendix) plus an appropriate background to the peaks. To reduce the number of free parameters in the fit we first determined the shape parameters C_4, C_5 and C_6 from fits to the 815.8 and 867.8 keV peaks for both angles. With different fit-intervals (44–96 channels) we obtained shape parameters which varied rather strongly (up to 40%); the anisotropy of the 815.8 and 867.8 keV transitions, however, remained almost constant (maximum difference 0.01). We then made fits to the peaks at 751.8, 815.8, 867.8 and 951.1 keV with the shape parameters maintained at the maximum or the minimum value as obtained from the fits to the 815.8 and 867.8 keV peaks. The anisotropies which resulted from all possible combinations of C_4, C_5 and C_6 differed by less than 0.009 for all transitions except the 951.1 keV line where the maximum change

was 0.05. This shows that the influence of the actual values of the shape parameters on the anisotropy is small.

The peak areas of the only partially resolved doublet of the 919.6 and 925.2 keV transitions were obtained from a fit of the sum of two modified Gaussians with equal line width. In addition to C_4, C_5 and C_6 maintained, we also kept fixed the energy difference of both gamma transitions which was measured by Baer et al. [22] to be 5.59 ± 0.23 keV. Within this energy region the anisotropy of the 919.6 keV transition varied by less than 0.002 and that of the 925.2 keV transition by less than 0.03. The fit with the smallest χ^2 was realized at an energy difference of 5.55 keV, which confirms Baer's value.

Table 2
Anisotropy $[W(180°) - W(90°)]/W(90°)$ of gamma rays in coincidence with the 1596.6 keV transition in ^{140}Ce

Energy [keV]	Anisotropy
751.8	-0.000 ± 0.032
815.8	-0.115 ± 0.016
867.8	-0.092 ± 0.018
919.6	0.113 ± 0.062
925.2	0.533 ± 0.031
951.1	-0.284 ± 0.094

Our final results for the anisotropy of the six gamma transitions (Table 2) have been adopted in such a way that they cover all values obtained from the different fits with their statistical errors. Our errors therefore reflect not only the statistical uncertainties but also the influence of the particular shape chosen to analytically describe a peak.

The finite solid angle corrections for the Ge(Li) detector, $Q_2 = 0.979 \pm 0.002$ and $Q_4 = 0.931 \pm 0.006$, have been obtained by interpolation of values from the tables calculated by Camp et al. [25]. The quoted errors arise from the uncertainties in the dimensions of the Ge(Li) detector and the source-detector distance. The interpolation from the tables of Yates [26] yielded $Q_2 = 0.872 \pm 0.004$ and $Q_4 = 0.621 \pm 0.009$ for the NaI(Tl) detector. The effects of the finite size of the source, scattering and absorption in the source and scattering from one detector into the other have been taken into account.

The finite solid angle corrections were used to calculate the anisotropy as a function of mixing ratio for different spin values X of a $X \rightarrow 2 \rightarrow 0$ cascade (Figs. 6–11). The F-coefficients were taken from the tables of Appel [27]. The possible multipolarities and mixing ratios of the first transition (the $2^+ \rightarrow 0^+$ transition must be of pure $E2$ type) were calculated from the comparison of theoretical (Sliv et al. [28]) and experimental K-conversion coefficients (as quoted by Baer et al. [22]). Our experimental anisotropy then allowed us to deduce spin assignments and mixing ratios which are listed in Table 3.

3.2.1.2. Discussion of spin assignments and mixing ratios. The following discussion is based on the well-established J^π assignments of 2^+ and 4^+ to the 1596.6 and 2083.6 keV levels, respectively. Some of our results (Table 3) have been confirmed very recently by Wiedenbeck et al. [29].

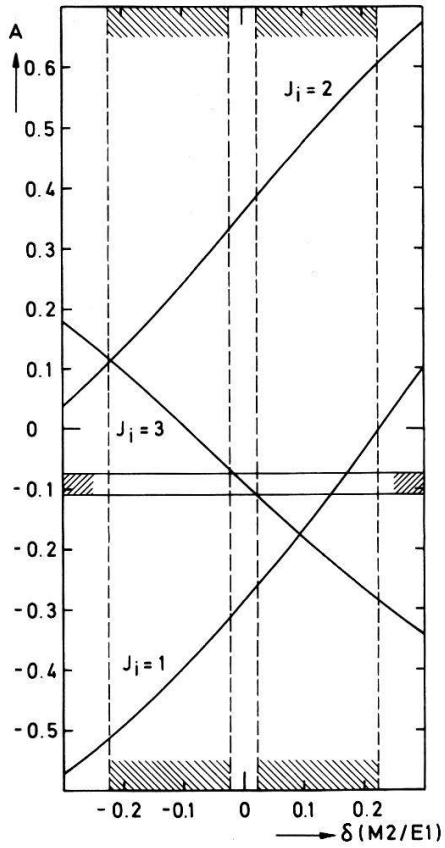

Figure 6
Anisotropy A of the 867.8 keV transition in coincidence with the 1596.6 keV gamma ray as a function of mixing ratio δ. J_i is the spin of the initial level. The hatched regions denote the mixing ratio compatible with the K-conversion coefficient quoted by Baer et al. [22] and the anisotropy from the present work, respectively.

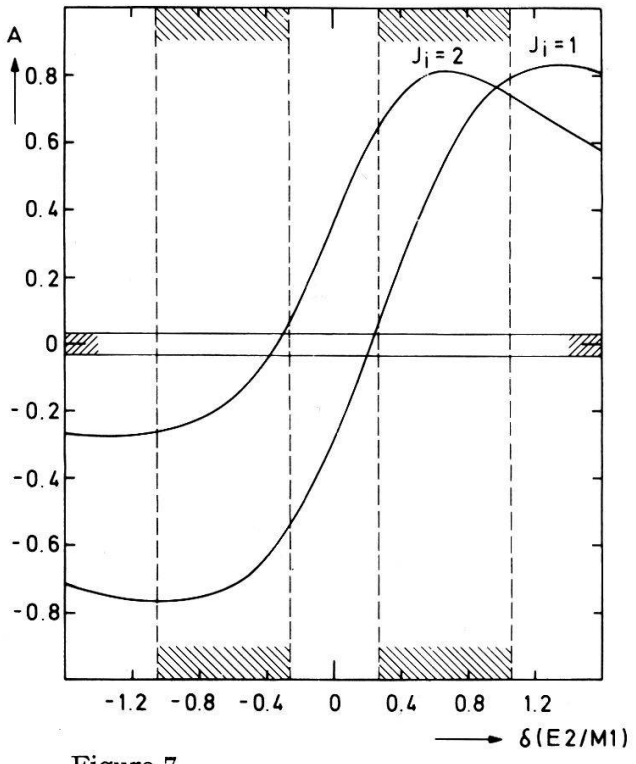

Figure 7
Anisotropy A of the 751.8 keV transition. See caption to Figure 6.

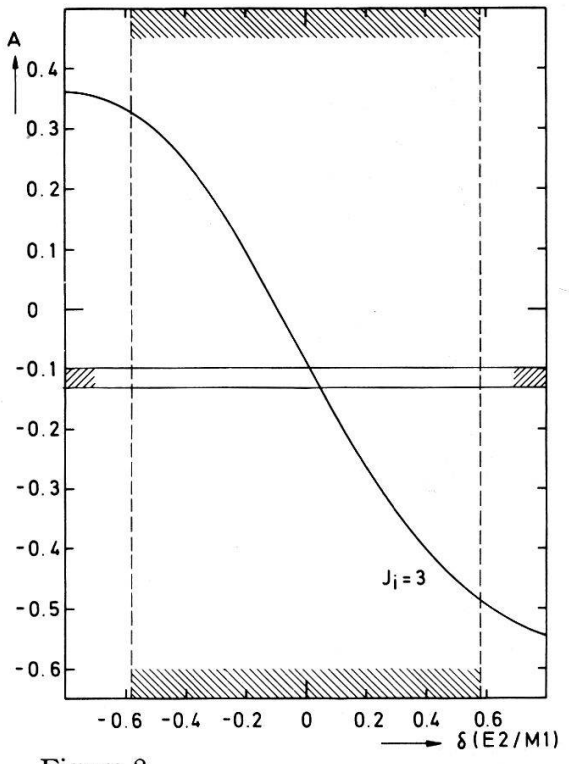

Figure 8
Anisotropy A of the 815.8 keV transition. See caption to Figure 6.

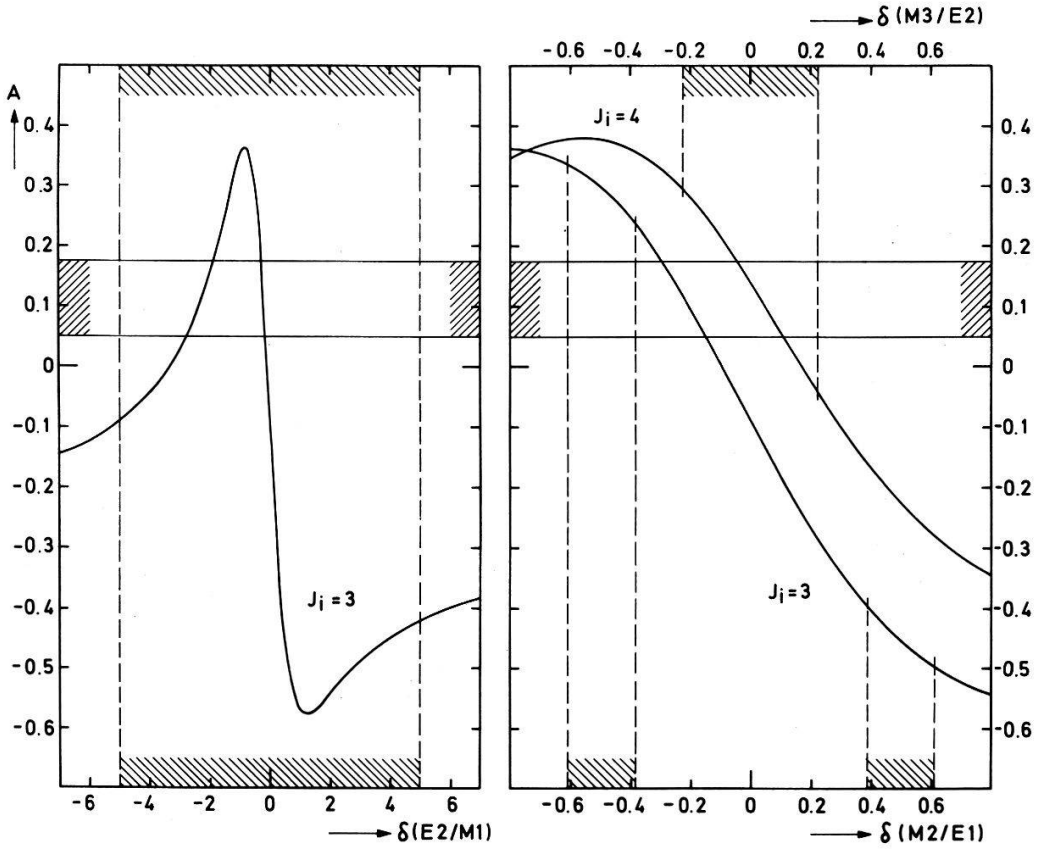

Figure 9
Anisotropy A of the 919.6 keV transition. See caption to Figure 6.

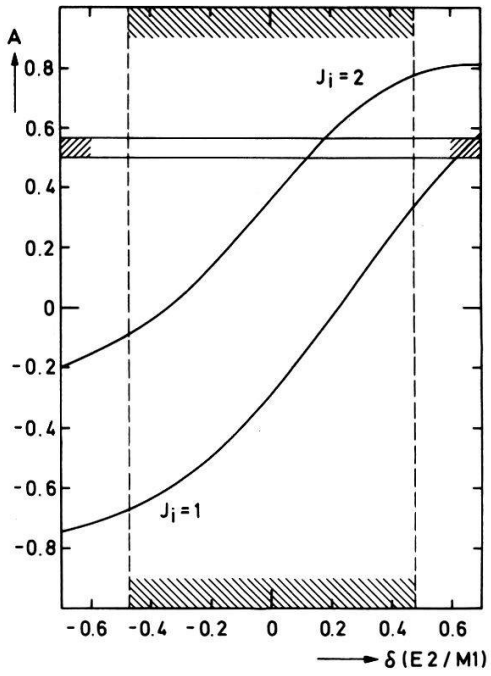

Figure 10
Anisotropy A of the 925.2 keV transition. See caption to Figure 6.

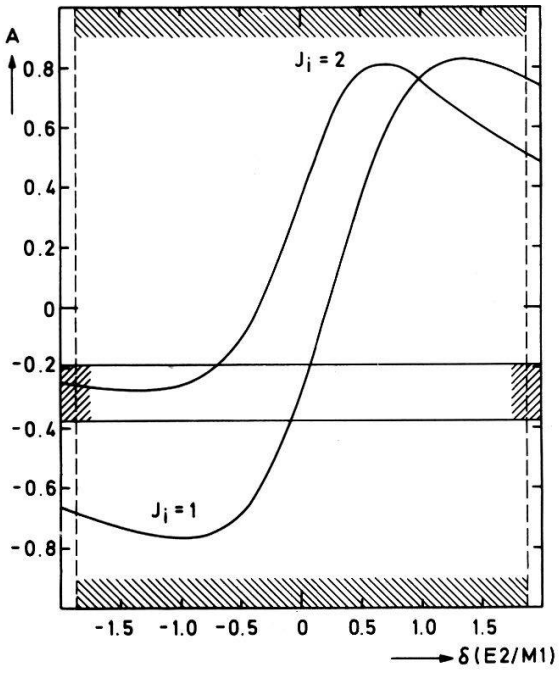

Figure 11
Anisotropy A of the 951.1 keV transition. See caption to Figure 6.

2464.4 keV level. The K-conversion coefficient of the 867.8 keV transition is compatible only with an $E1 + M2$ multipolarity, thus allowing $J^\pi = 1^-, 2^-, 3^-$ for the 2464.4 keV level. Our anisotropy measurement (Fig. 6) definitely excludes $J = 2$ but does not favour one of the remaining possibilities. There exist, however, other arguments against the 1^- assignment. Firstly, the log ft value of 8.5 [22] for this level would be very low for a second forbidden beta decay, but agrees well with other values for allowed transitions to the 3^- octupole state. Furthermore, we were able to measure the intensity of the cross-over transition to the groundstate (see 3.2.2). If the 2464.4 keV level has $J^\pi = 1^-$ then the 2464.4 and 867.8 keV gamma rays are both $E1$ transitions and from the branching ratio follows $B(E1, 867.8\text{ keV})/B(E1, 2464.4\text{ keV}) = (1.34 \pm 0.20) \cdot 10^4$. This very high value also disfavours the 1^- assignment. We therefore conclude that the 2464.4 keV level has $J^\pi = 3^-$ and that the 867.8 keV transition is a pure $E1$ transition [$\delta(M2/E1) = 0.00 \pm 0.02$ [2])].

2348.8 keV level. The K-conversion coefficient of the groundstate transition is compatible only with pure $M1$ or $E2$ multipolarity, thus restricting J^π to 1^+ or 2^+.

Table 3

Results of anisotropy measurements in ^{140}Ce

Level energy [keV]	J^π	Gamma ray energy [keV]	Multipolarity	Mixing ratio†)
2348.4	2^+	751.8	$M1 + E2$	-0.35 ± 0.04
2412.4	3^+	815.8	$M1 + E2$	0.03 ± 0.02
2464.4	3^-	867.8	$E1 + M2$	0.00 ± 0.02
2516.1	3^+	919.6	$M1 + E2$	-0.22 ± 0.07
				or -2.36 ± 0.45
	4^+		$E2 + M3$	0.03 ± 0.08
2521.8	2^+	925.2	$M1 + E2$	0.15 ± 0.03
2547.5	1^+	951.1	$M1 + E2$	0.00 ± 0.08
	2^+		$M1 + E2$	$\leqslant -0.67$

†) The sign is defined according to the formulas of Biedenharn and Rose [30].

This fixes the multipolarity of the 751.8 keV transition to the 1596.6 keV (2^+) level as $M1 + E2$, in agreement with the K-conversion coefficient. Our anisotropy measurement does not definitely rule out the 1^+ assignment to the 2348.8 keV level (Fig. 7). If we accept, however, the $J^\pi = 3^+$ assignment to the 2412.4 keV level (see discussion of this level later) then the $M1$ multipolarity of the 64.1 keV (2412.4 → 2348.8 keV) transition fixes $J^\pi = 2^+$ to the 2348.8 keV level. Our anisotropy measurement then yields $\delta(E2/M1) = -0.35 \pm 0.04$.

2412.4 keV level. The K-conversion coefficient of the 815.8 keV transition is compatible with the multipolarities $E1 + M2$, $M1 + E2$ and $E2 + M3$. Further information can be obtained from the 328.8–487.0 keV cascade proceeding to the 1596.6 keV (2^+) level via the 2083.6 keV (4^+) state. Angular correlation measurements [31–36] positively determined the spin sequence as 3–4–2 and from the K-conversion coefficient follows $M1$ multipolarity of the 328.8 keV transition. Therefore the

[2]) In the present work the sign of δ is defined according to the formulas of Biedenharn and Rose [30].

2412.4 keV level must have $J^\pi = 3^+$ and the 815.8 keV transition is of $M1$ multipolarity. From our anisotropy measurement (Fig. 8) then follows $\delta(E2/M1) = 0.03 \pm 0.02$.

This result helps to clarify the situation of conflicting A_2 and A_4 values reported in various papers. Our anisotropy is in accordance with the value deduced from the measurements done by Black et al. [31] and also compatible with the result of Bishop et al. [37]. The values deduced from the results of Bolotin et al. [32], Kelley et al. [33] and Bannerman et al. [38], however, strongly disagree with our value.

2516.1 keV level. The K-conversion coefficients of the 919.6 keV transition to the 1596.6 keV (2^+) level and of the 432.5 keV transition to the 2083.6 keV (4^+) level are both consistent with $E1 + M2$, $M1 + E2$ and $E2 + M3$ multipolarity, thus restricting J^π to 2^+, $3^\pm$ or 4^+. The 2^+ assignment is improbable because the groundstate transition is absent. From our anisotropy measurement (Fig. 9) we conclude that the 919.6 keV transition is most probably not an $E1$ transition and therefore reject $J^\pi = 3^-$. The mixing ratios for the remaining multipolarities are listed in Table 3.

2521.8 keV level. The K-conversion coefficient of the groundstate transition is compatible only with pure $M1$ or $E2$ multipolarity, thus allowing $J^\pi = 1^+$ or 2^+ in agreement with α_K of the 925.2 keV transition which is compatible with a $M1$ multipolarity. Since the 109.4 keV transition between the 2521.8 and 2412.4 keV (3^+) levels is a $L = 1$ transition the spin of both states can differ at most by 1, thus eliminating $J = 1$ for the 2521.8 keV level. Our anisotropy measurement also favours $J^\pi = 2^+$ (Fig. 10) and we obtain $\delta(E2/M1) = 0.15 \pm 0.03$.

2547.5 keV level. The K-conversion coefficient of the groundstate transition is compatible only with pure $M1$ or $E2$ multipolarity, so $J^\pi = 1^+$ or 2^+. This is in agreement with α_K of the 951.1 keV transition which allows a $M1$ multipolarity. Our anisotropy measurement (Fig. 11) yields $\delta(E2/M1) = 0.00 \pm 0.08$ for $J^\pi = 1^+$ and $\delta(E2/M1) \leqslant -0.67$ for $J^\pi = 2^+$.

3.2.2. E3 groundstate transition from the 2464.4 keV level

The only possibility of identifying a transition as the $E3$ groundstate transition is to compare its energy with the energy of the 3^- level. In the case of ^{140}Ce this method requires the energy measurement of a very weak 2.5 MeV gamma ray with an accuracy of a few tenths of keV since the level energy is known to within ± 0.3 keV [22, 39]. This can only be done with a careful energy calibration involving the investigation of nonlinearities of the spectrometer system to exclude systematic errors.

To avoid this procedure, we decided to measure the energy of the gamma ray in question relative to that of the sum peak of the $3^- \rightarrow 2^+ \rightarrow 0^+$ cascade. With equal count rates in the detector both radiations are subject to the same systematic changes in the electronic system, which therefore cancel out. To ensure a high probability of summing, the source must be placed very close to the detector, as opposed to the case of the search for the $E3$ transition where the source-detector distance has to be large in order to prevent summing. These different geometries cause a shift of the peaks in relation to each other due to charge-carrier trapping. We have investigated this effect [40] and found that it increases linearily with the gamma ray energy. Therefore the relative peak positions are not affected and no systematic error arises from this peak shift.

3.2.2.1. Measurements and results. We used a gamma ray spectrometer system with a 40 cm^3 true coaxial Ge(Li) detector (Nuclear Enterprises GD 602) which is sketched in Figure 12. The spectrum was digitally stabilized using the 2348.8 and 2522.2 keV peaks below and above the expected 2464.4 keV peak. The full-energy peak efficiency of the detector was measured with known calibrated sources of ^{60}Co and ^{137}Cs and an uncalibrated ^{24}Na source and is well represented by the function $a \cdot \exp(-b \cdot \ln E)$. The constants a and b were determined from a least-squares fit and used for interpolation.

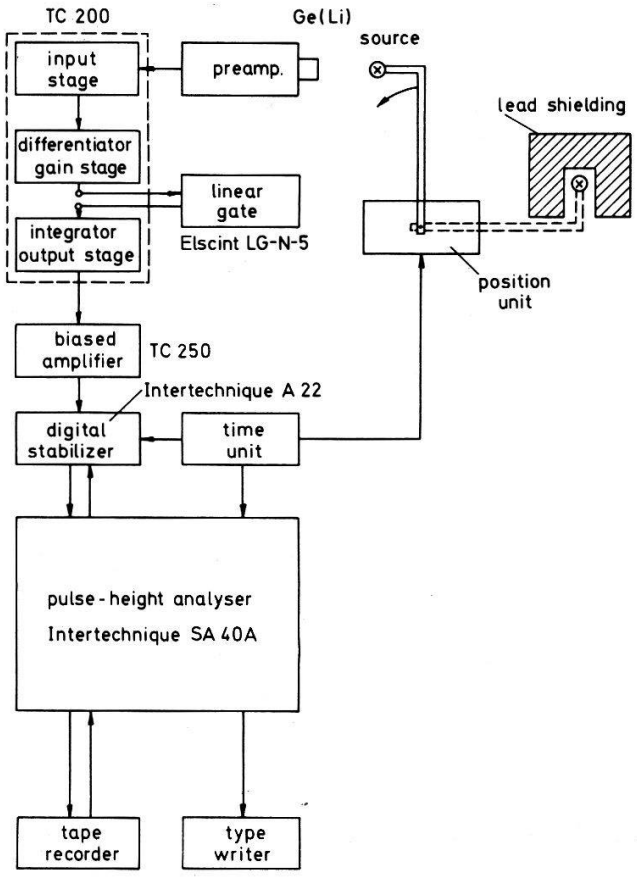

Figure 12
Block diagram of the electronics used for the gamma ray spectroscopy of the decays $^{140}La \rightarrow {}^{140}Ce$ and $^{160}Tb \rightarrow {}^{160}Dy$. The linear gate has been used only in the search for the $3^- \rightarrow 4^+$ transition in ^{140}Ce.

We prepared pairs of sources with activities of about 1 mCi and 0.2 μCi, respectively, in order to measure both the sum peak of the $3^- \rightarrow 2^+ \rightarrow 0^+$ cascade and the $3^- \rightarrow 0^+$ transition with equal count rates in the detector. This condition was achieved by placing the weak source as close as possible to the front face of the detector and adjusting the distance of the strong source (typically to 82 cm). The geometrical details of both arrangements are shown in Figure 13.

The 'direct' spectrum (with the strong source far from the detector to prevent summing) was recorded in periods of 40 min each. The source then was automatically removed and placed behind a 10 cm lead shielding (Fig. 12) to measure the background. Each source was measured for three half-lives, the source-detector distance was decreased after each half-life in order to regain the initial count rate in the detector. At regular intervals we also measured the sum spectrum with the weak source placed close to the detector.

After summing the spectra, the background, corrected for the counting time, was subtracted. Figure 14 shows the part of the gamma spectrum of ^{140}Ce with the sum peak of the $3^- \rightarrow 2^+ \rightarrow 0^+$ cascade. Figure 15 shows the same energy region measured with the source far away from the detector showing the full-energy peak of the $E3$ groundstate transition. The intensities of both sum peaks $815.8 + 1596.6$ and $867.8 + 1596.6$ keV are in excellent agreement with the values calculated using the single gamma ray intensities [22], the solid angle and the efficiency of the detector. From a brief inspection of both spectra one immediately concludes that the 2464.4 keV peak in the 'direct' spectrum cannot be the result of a summing, since the sum peak of the 815.8–1596.6 keV cascade, which would be four times more intense, is absent.

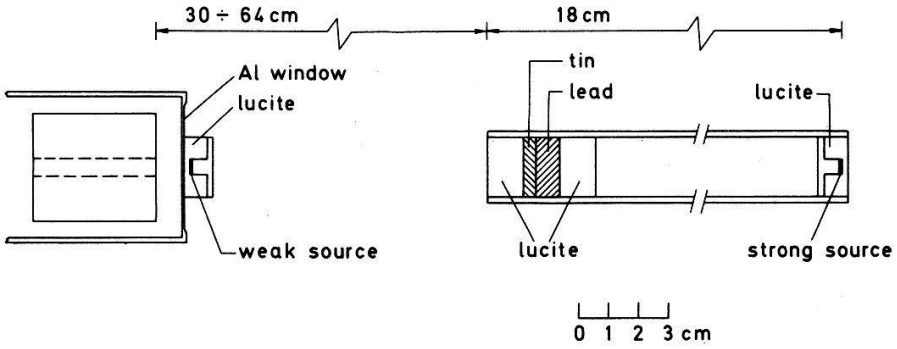

Figure 13
Source to detector geometry for the measurement of the $E3$ transition and the sum spectrum.

For the intensity determination of the 2464.4 keV transition we first fitted a modified Gaussian (see appendix) with appropriate background to the 2348.8 and 2522.2 keV peaks to obtain the shape parameters C_4, C_5 and C_6 and the line width. We then fitted the 2464.4 keV peak with the shape parameters and the line width kept fixed at the values obtained from interpolation to the correct energy. Constant background resulted in a poor fit; both linear and parabolic background, however, yielded equally good fits and from the average of both peak areas we deduced an intensity ratio $I(2464.4 \text{ keV})/I(2522.2 \text{ keV}) = (2.74 \pm 0.35) \cdot 10^{-3}$. The quoted error includes both statistical error and the variation arising from the different background assumptions. The summing in the detector was calculated to be 1.3% of the measured intensity and has been accounted for; the pile-up was negligible.

The sum spectrum was handled in a similar manner. We again determined the shape parameters of the 2348.8 and 2522.2 keV peaks and interpolated to 2464.4 keV. Since the $867.8 + 1596.6$ keV sum peak includes an amount of the cross-over gamma rays, this fraction was subtracted prior to the fit of a modified Gaussian with the shape parameters and the line width maintained. All assumptions of constant, linear and parabolic background gave equally good fits.

The positions of the 2464.4 keV peak obtained with linear and parabolic background, and those of the sum peak obtained with all three background assumptions, were averaged to get the final positions. The errors were adopted in such a way that they cover all other values. With the energy calibration scale of the spectra we obtained

$$E(\text{direct peak}) - E(\text{sum peak}) = 230 \pm 200 \text{ eV}.$$

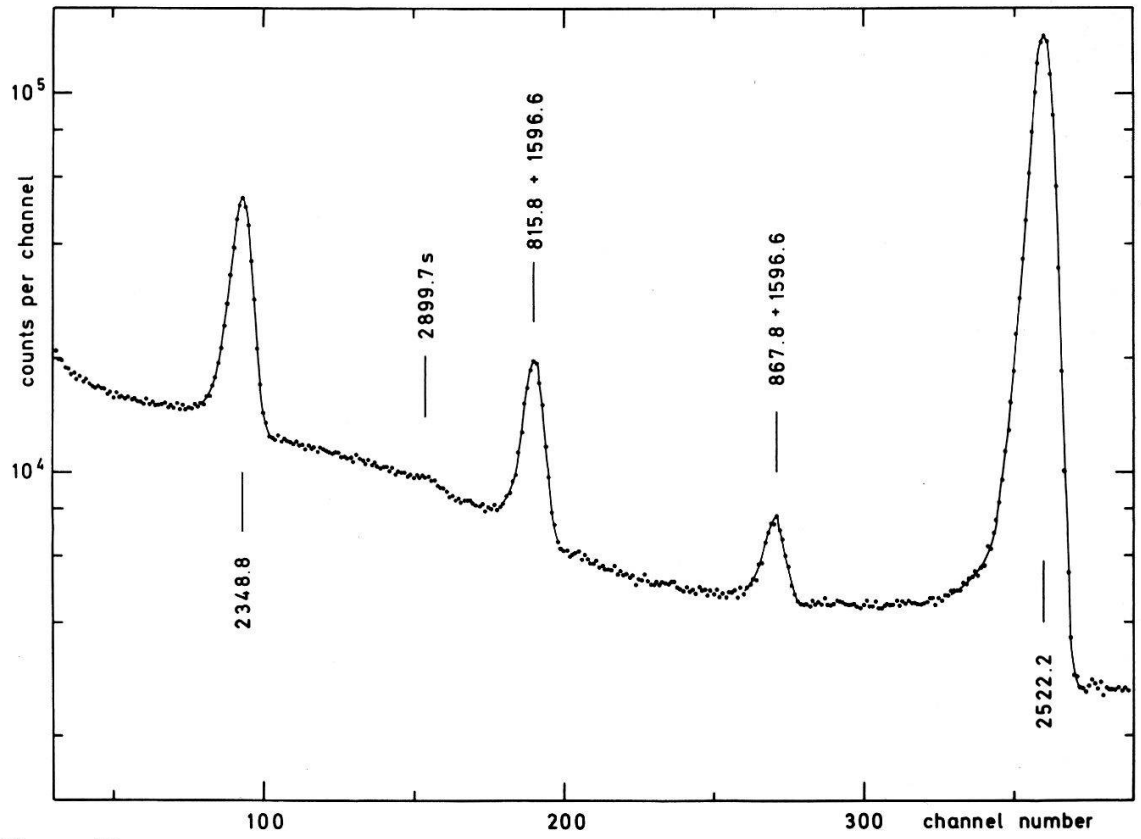

Figure 14
Partial gamma ray spectrum of ^{140}Ce showing the sum peak of the $3^- \rightarrow 2^+ \rightarrow 0^+$ cascade. Energies are in keV. s: single-escape peak.

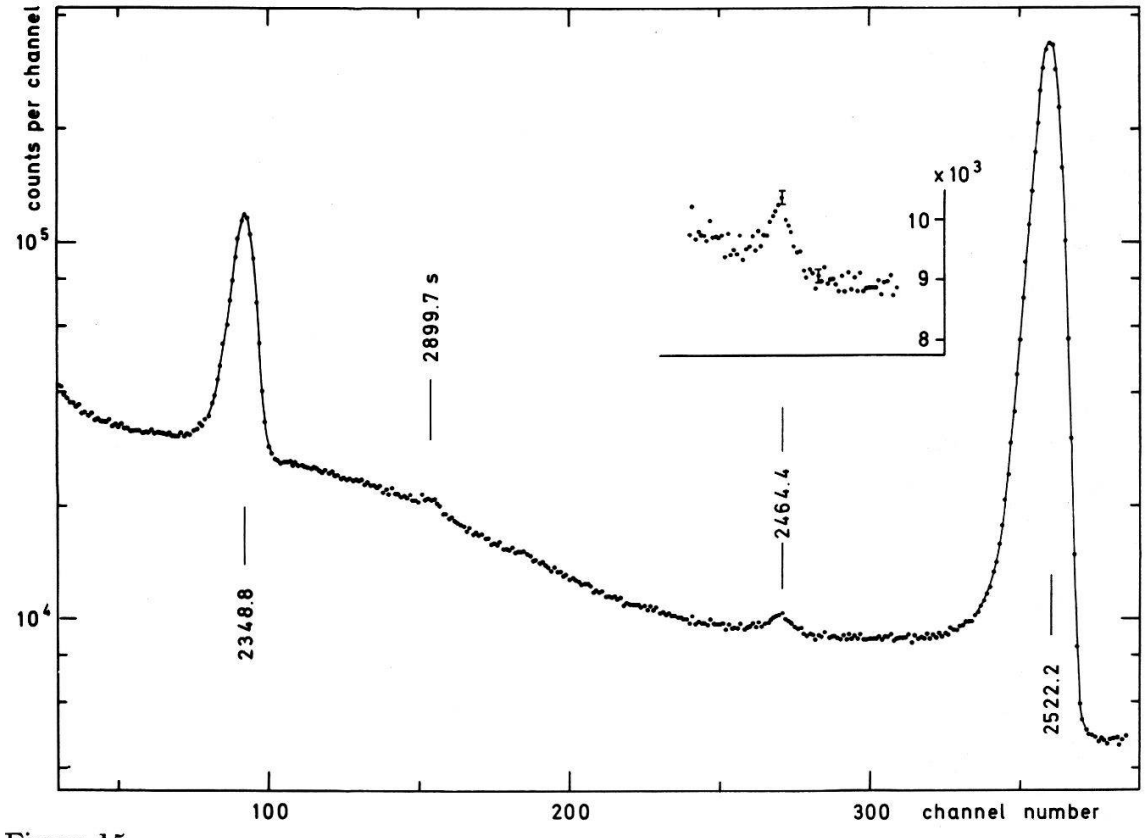

Figure 15
Partial gamma ray spectrum of ^{140}Ce showing the $3^- \rightarrow 0^+$ transition. Energies are in keV. s: single-escape peak.

3.2.2.2. Discussion. Since the energy difference between the sum peak of the $3^- \rightarrow 2^+ \rightarrow 0^+$ cascade and the direct peak is compatible with zero, we conclude that the latter arises from the $E3$ groundstate transition. Combining the intensity ratios $I(2522.2\ \text{keV})/I(867.8\ \text{keV}) = 0.624 \pm 0.044$ [22] and $I(2464.4\ \text{keV})/I(2522.2\ \text{keV})$ from the present work we calculate an $E3/E1$ branching ratio of $(1.71 \pm 0.25) \cdot 10^{-3}$ which is $(8.4 \pm 1.2) \cdot 10^3$ times the single particle estimate. The reduced transition probability $B(E3)$ has been determined from inelastic electron scattering by Pitthan [41] to be 26 ± 3 single particle units. Using this value, we derive from our $E3/E1$ branching ratio that the $E1$ transition is 330 ± 60 times retarded with respect to the single particle estimate. We wish to emphasize that this is the fastest $3^- \rightarrow 2_1^+$ transition yet known (see Section 4).

Recently, Ardisson et al. [42] determined the $E3/E1$ branching ratio to be $5.0 \cdot 10^{-3}$. This value disagrees with our result but we cannot find any reason for this discrepancy. The 2494 keV transition reported by the same authors [42] has not been observed in our experiment. If there is a line of this energy its intensity must be smaller by a factor of about 10 than quoted by Ardisson et al. [42].

3.2.3. Search for the 380.8 keV $3^- \rightarrow 4^+$ transition

In their extensive study of the ^{140}La decay, Baer et al [22] give an upper limit of $1.86 \cdot 10^{-2}$ for the branching ratio $I(3^- \rightarrow 4^+)/I(3^- \rightarrow 2^+)$, which is 0.22 times the single particle estimate. From gamma spectroscopy on neighbouring nuclei this ratio is found to lie in the region of about 0.1 to 1 single particle units. Thus we decided to make a more thorough search for the $3^- \rightarrow 4^+$ transition.

3.2.3.1. Measurements and results. The measurements were performed with a planar Ge(Li) detector of 3.5×0.75 cm^3 active volume. In addition to the previously used electronic equipment we introduced a linear gate (Elscint LG-N-5) between the first differentiator and the integrator of the main amplifier (Fig. 12). This reduced the count rate at an early stage in the amplifier where the pulses are short and thus decreased pile-up effects in the later stages where the pulses are shaped without deterioration of the resolution.

The efficiency calibration of the detector was carried out using the more intense gamma transitions of a ^{160}Tb source; the intensities were taken from Ludington et al. [43]. Again the efficiency curve is well represented by the function $a \cdot \exp(-b \cdot \ln E)$; the constants a and b were obtained from a least-squares fit to the data and used for interpolation.

Three sources each of about 4 mCi activity were sealed in lucite housings, the dimensions of which can be seen in Figure 13.

The gamma spectrum was measured in periods of 30 min each alternating with the background (source behind a 10 cm lead shielding). The spectrum was digitally stabilized using the stronger 328.8 and 487.0 keV peaks as references. The spectrum in the energy region of 300–500 keV, corrected for background, is displayed in Figure 16.

The peak areas of the strong peaks at 328.8, 432.5 and 487.0 keV were determined from fits of a modified Gaussian (see appendix) plus background. We then fitted a modified Gaussian plus parabolic background with the shape parameters C_4, C_5, C_6 and the line width kept at the interpolated values to the 397.8 keV peak. Since no peak is visible at 380.8 keV we are only able to give an intensity limit for this transition.

It was obtained from the fit of a modified Gaussian (see appendix) plus parabolic background, to the spectrum around the expected peak, with all parameters kept at the interpolated values except the peak area and the coefficients of the background

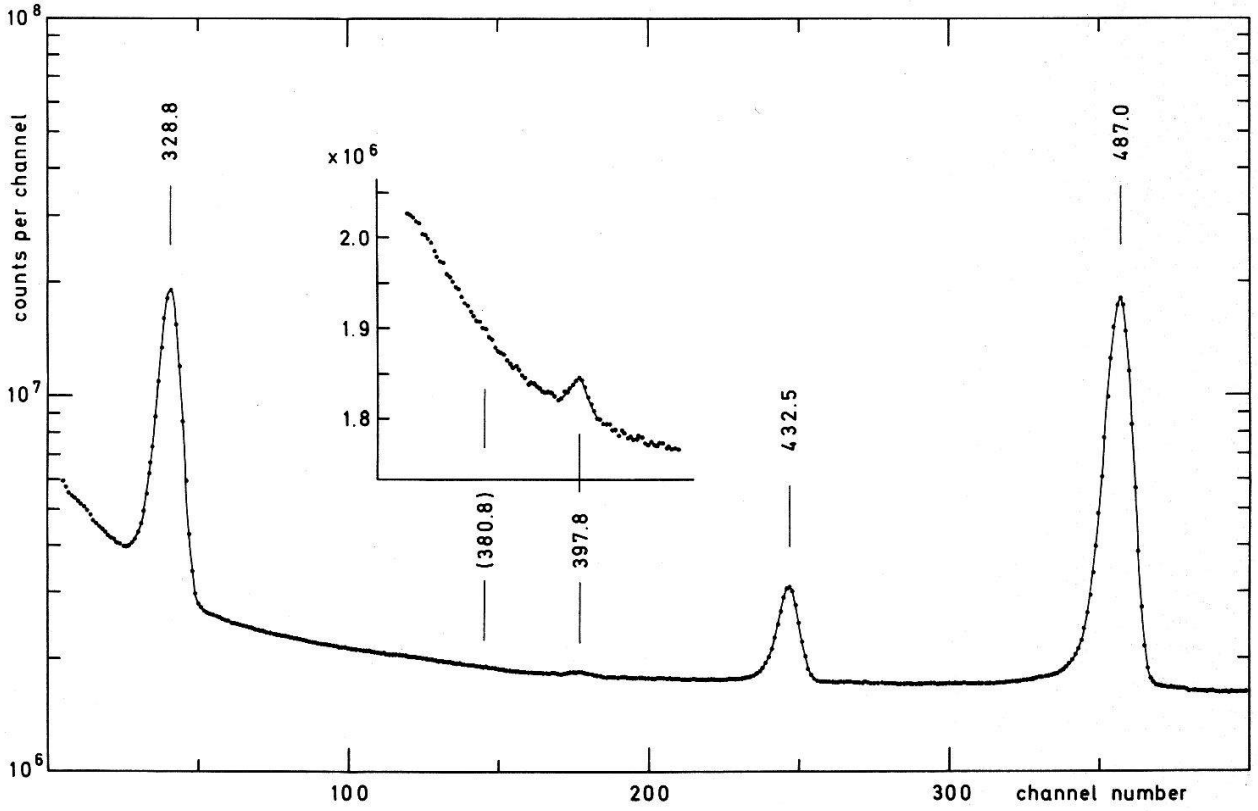

Figure 16
Partial gamma ray spectrum of ^{140}Ce showing the region around the possible $3^- \rightarrow 4^+$ transition of 380.8 keV. Energies are in keV.

distribution. This fit was done for different fit intervals and yielded peak areas compatible with zero in most cases. The maximum value was about twice its statistical error and the sum of both has been used as an upper limit for the peak area.

The relative gamma ray intensities measured in the present investigation are listed in Table 4.

Table 4

Relative gamma ray intensities in the ^{140}La $\rightarrow$ ^{140}Ce decay

Energy†) [keV]	Rel. intensity‡) [%]
328.8	21.7 ± 0.4
380.8	< 0.0072
397.8	0.076 ± 0.003
432.5	3.23 ± 0.06
487.0	49.4 ± 0.9

†) Taken from Baer et al. [22].
‡) Normalized to I(487.0 keV) = 49.4% [22].

3.2.3.2. Discussion. Our intensities agree very well with the results of Baer et al. [22] but are of considerably improved accuracy. The 380.8 keV $3^- \rightarrow 4^+$ transition has not been observed and we set an intensity limit of $7.2 \cdot 10^{-5}$ relative to the 1596.6 keV transition. Using the intensity of the $3^- \rightarrow 0^+$ transition from the present work and the excitation probability $B(E3)$ [41] we calculate $B(E1, 3^- \rightarrow 4^+) < 5.5 \cdot 10^{-5}$ single particle units, a limit well compatible with the values which have been observed for other nuclei [6].

It is interesting to compare the reduced transition probabilities $B(E1)$ of the $3^- \rightarrow 2^+$ and $3^- \rightarrow 4^+$ transitions. In most nuclei both quantities are of the same order of magnitude [6]; for ^{140}Ce, however, we deduce from our measurements a ratio $B(E1, 3^- \rightarrow 4^+)/B(E1, 3^- \rightarrow 2^+) < 1.6 \cdot 10^{-2}$. This value is smaller by a factor of 10 than the smallest value yet known (^{124}Te: 0.160 ± 0.003 [6]) and indicates a considerably different structure between the first 2^+ and 4^+ levels.

3.3. The nucleus ^{160}Dy

The decay of ^{160}Tb to levels in ^{160}Dy has been the subject of many investigations; one of the most extensive being that of Ludington et al. [43]. The results of all measurements have confirmed the existence of two 3^- levels at 1286.7 and 1399.0 keV (see Fig. 17). Ludington et al. [43] observed a transition with an energy of 0.9 ± 0.5 keV less than the energy of the first 3^- level and which they tentatively interpreted as the groundstate transition. We therefore reinvestigated this particular transition in order to decide whether it is the $E3$ crossover transition or not. For this purpose we compared the energy of the full-energy peak with that of the sum peak of the $3^- \rightarrow 2^+ \rightarrow 0^+$ cascade. With the same techniques we searched for the $E3$ groundstate transition from

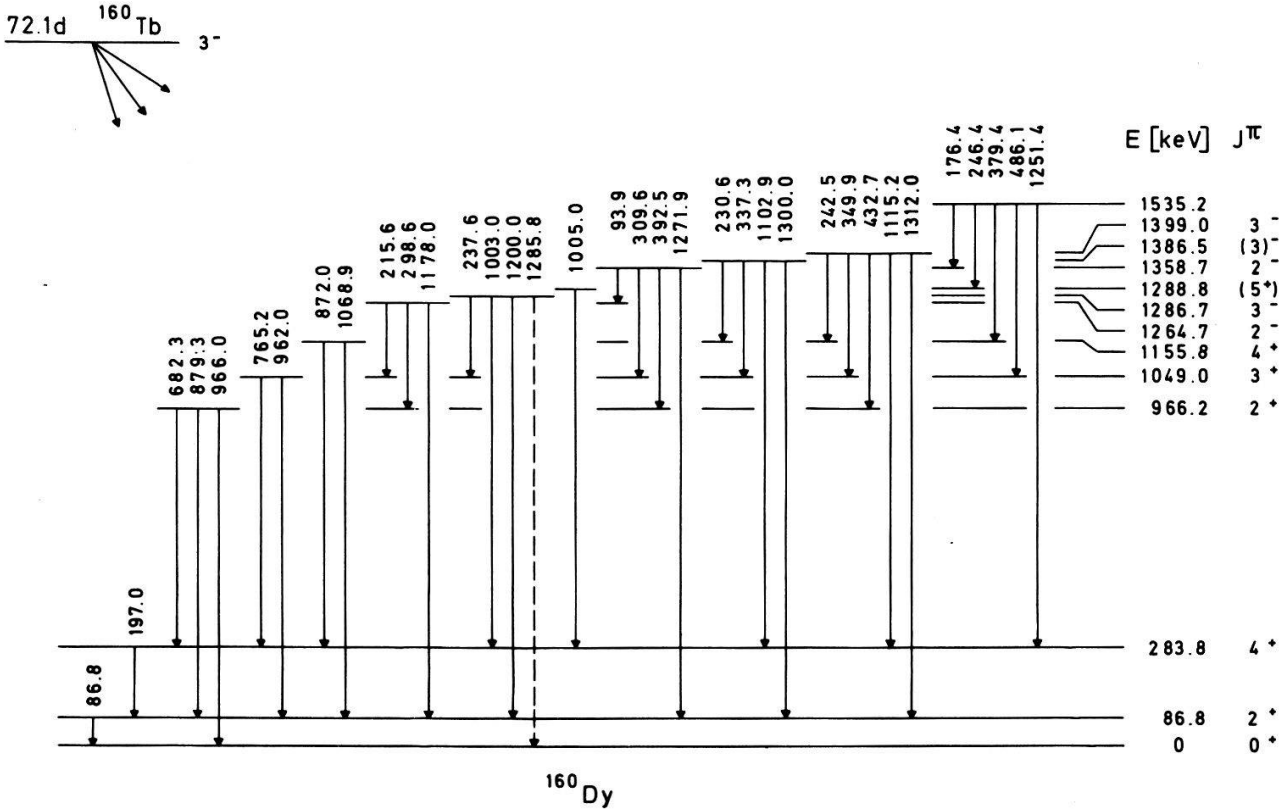

Figure 17
Decay scheme of ^{160}Tb according to Ludington et al. [43].

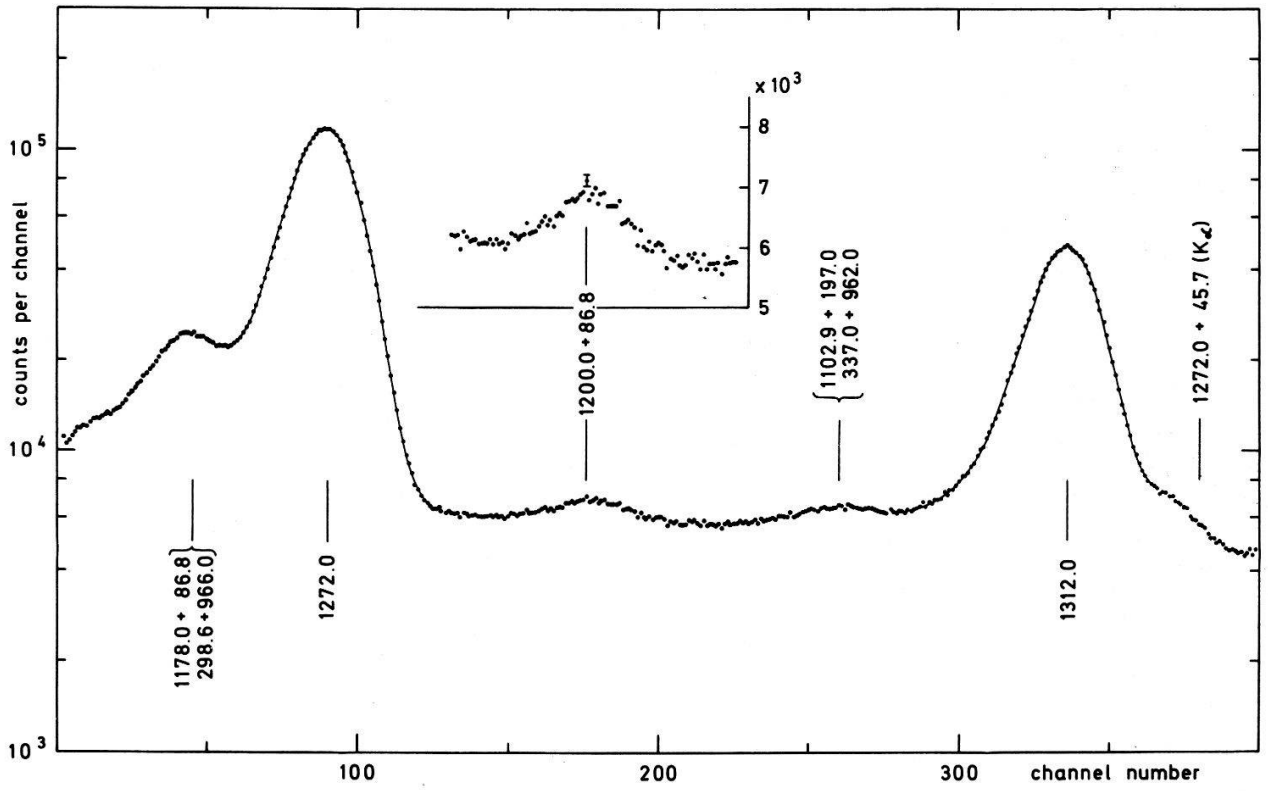

Figure 18
Partial gamma ray spectrum of ^{160}Dy showing the sum peak of the $3^- \rightarrow 2^+ \rightarrow 0^+$ cascade originating from the first 3^- level at 1286.7 keV. Energies are in keV.

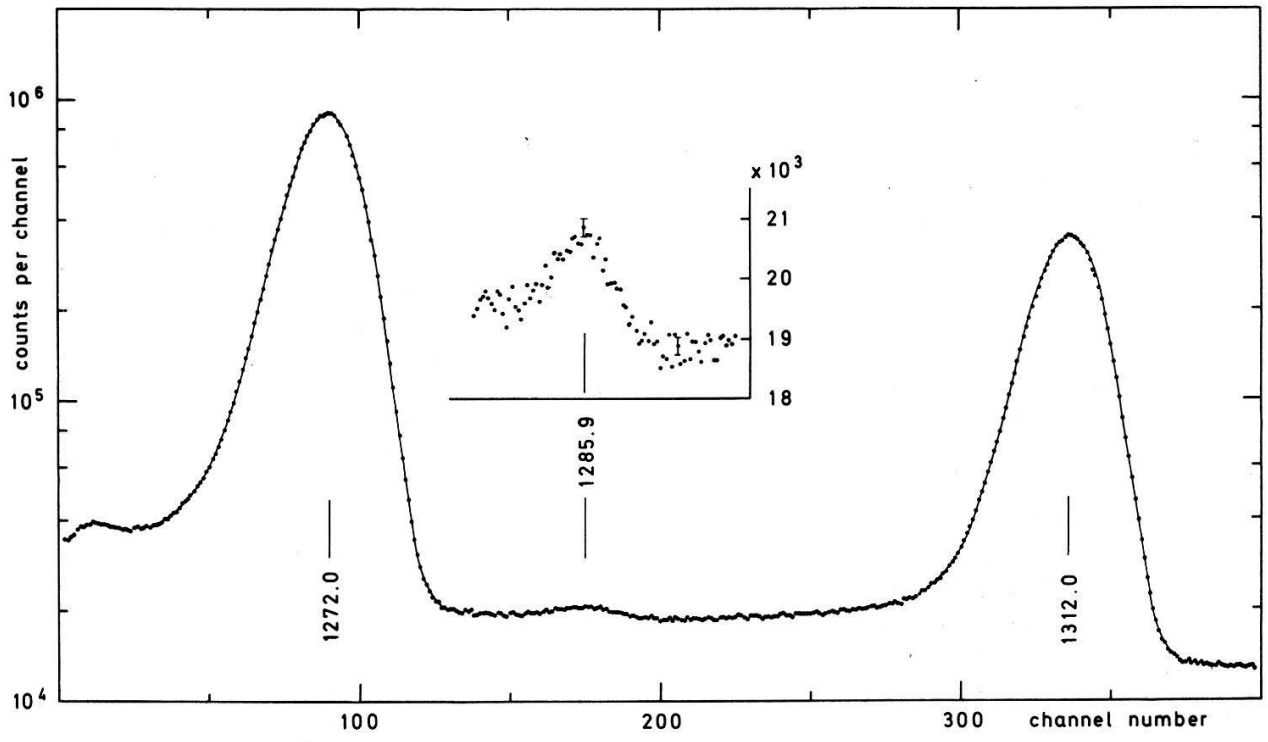

Figure 19
Partial gamma ray spectrum of ^{160}Dy showing the region around the possible $E3$ groundstate transition from the first 3^- level at 1286.7 keV. Energies are in keV.

the second 3^- level. Preliminary results have been reported at the 1969 autumn meeting of the Swiss Physical Society [23].

3.3.1. Measurements and results. The measurements were performed with a 40 cm^3 coaxial Ge(Li) spectrometer system (Fig. 12). The spectra were digitally stabilized using the 1272.0 and 1312.0 keV peaks for the investigation of the 1286.7 keV transition; in the case of the 1399.0 keV transition the 1312.0 keV line and the peak of a pulse generator (SES, P 100) fed into the test input of the preamplifier were used for stabilization.

The sources were produced by neutron activation of 99.999% natural Tb_2O_3 [3]) at the reactor DIORIT of the EIR in Würenlingen, Switzerland. After an irradiation of about one day two sources of about 0.8 mCi and 5 μCi activity were sealed in lucite housings. The geometrical details were the same as shown in Figure 13 except that we changed the thickness of the lead absorber to 8 mm and the source-detector distance to 17.0 cm for the 1286.7 keV and 11.5 cm for the 1399.0 keV transition.

The measurements were carried out in an analogous manner to that used for the $E3$ transition in ^{140}Ce, so we refer to Section 3.2.2.1 for further details. Figures 18 and 19 display the sum spectrum and the direct spectrum in the region around the possible

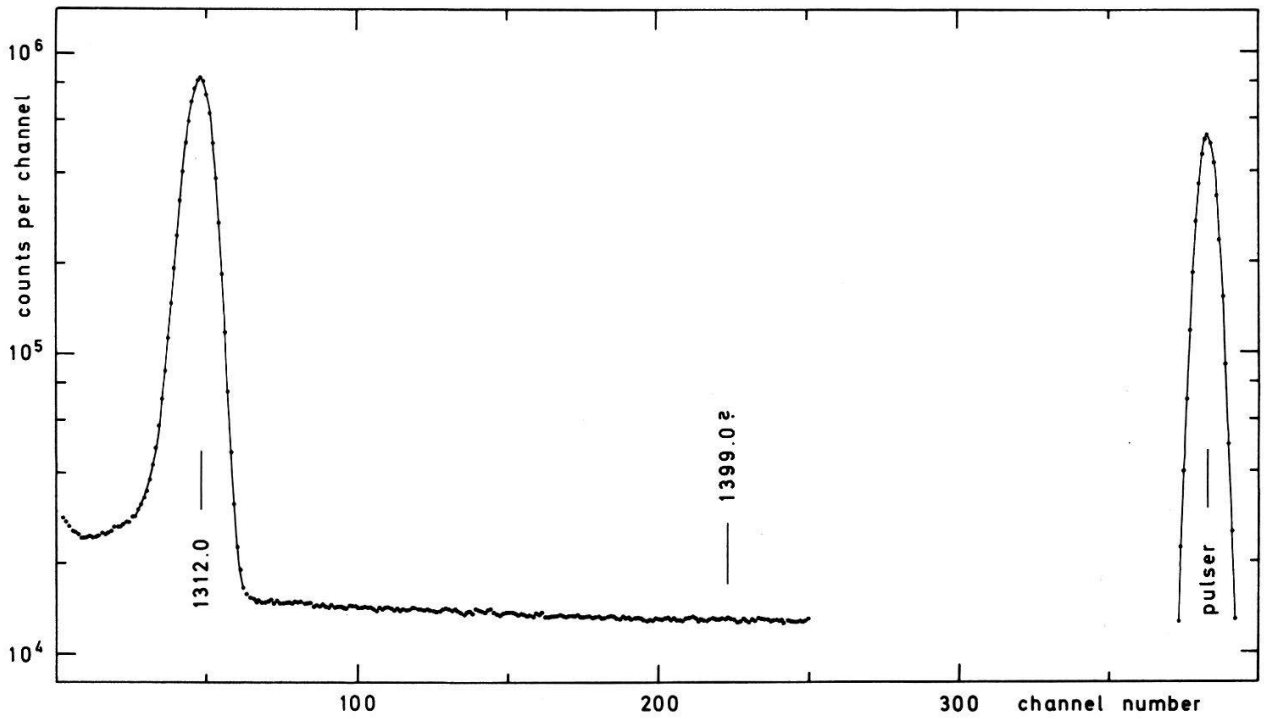

Figure 20
Partial gamma ray spectrum of ^{160}Dy showing the region around the possible $E3$ groundstate transition from the second 3^- level at 1399.0 keV. Energies are in keV.

1286.7 keV transition; in Figure 20 the direct spectrum around the possible 1399.0 keV transition is shown.

From fits of a modified Gaussian (see appendix) we obtained equal shape -parameters C_4, C_5 and C_6 and line widths for the following peaks in both the direct and the sum spectrum: 1272.0 and 1312.0 keV, 1312.0 and 86.8 + 1312.0 keV, pulse

[3]) Obtained from Koch-Light Laboratories Ltd., Poyle, Colnbrook, Buckinghamshire, England.

generator. We therefore averaged the shape parameters and the line width and repeated the fits with these parameters maintained to obtain the final positions of the reference peaks.

The sum peaks of the $3^- \rightarrow 2^+ \rightarrow 0^+$ cascades and the corresponding cross-over transitions (if present) were treated in the following manner.

1286.7 keV transition. Both the sum peak and the peak in the direct spectrum were fitted using a modified Gaussian (see appendix) with the shape parameters C_4, C_5 and C_6 and the line width maintained. The contribution of the direct spectrum was subtracted before analysis of the sum peak. Constant background resulted in a poor fit to the sum peak and unreasonable data for the direct peak. Both linear and parabolic background distributions yielded equally good fits, so we averaged the results to obtain the final positions. The errors were adopted in such a way that they cover the results from the fits with both linear and parabolic background. In the case of the sum peak the error was increased so that it includes also the position obtained with a constant background. With the energy calibration scale of the spectrum we obtained

$$E(\text{sum peak}) - E(\text{direct peak}) = 780^{+160}_{-300}\ \text{eV}.$$

The average of the peak areas resulting from the fits with linear and parabolic background was used to calculate the intensity ratio

$$I(\text{direct peak})/I(1272.0\ \text{keV}) = (2.06 \pm 0.13) \cdot 10^{-3}.$$

The quoted error includes both statistical error and the variation arising from the different background assumptions.

1399.0 keV transition. In the direct spectrum (Fig. 20) no peak appears at 1399.0 keV. The upper limit for the intensity of this transition was deduced from fits of a modified Gaussian (see appendix) to the spectrum with all parameters maintained except the peak area and the height of the constant background. The fit was done with different fit-intervals and yielded peak areas of zero within the statistical errors in all cases. The average of all values increased by the maximum statistical error was used to calculate an upper limit of $1.1 \cdot 10^{-4}$ for the branching ratio $I(1399.0\ \text{keV})/I(1312.0\ \text{keV})$.

3.3.2. Discussion. i) Our results for the energy and intensity of the possible groundstate transition from the first 3^- state at 1286.7 keV agree well with those reported by Ludington et al. [43]. Due to our higher accuracy we conclude from the energy difference between the sum peak of the $3^- \rightarrow 2^+ \rightarrow 0^+$ cascade and the 1286 keV transition, that the latter is not the $E3$ groundstate transition. According to the recent precise gamma ray measurements done by McAdams et al. [44] the 3^- level has an energy of 1286.69 ± 0.03 keV. Using this value we obtain an energy of $1285.91^{+0.30}_{-0.16}$ keV for the observed transition. This gamma line cannot be fitted into the decay scheme of ^{160}Tb and we have to introduce a new level in order to account for it. This might be the 1^- level at 1285.3 keV observed in the ^{160}Ho decay by Grigoriev et al. [45] who proposed that the 1285.9 keV transition depopulates this state. This suggestion, however, cannot be verified by our present data due to the very weak intensity of the 1285.9 keV transition.

ii) The intensity limit for the $E3$ groundstate transition from the second 3^- level at 1399.0 keV combined with the gamma ray intensities measured by Ludington et al. [43] allows us to calculate upper limits for the various branching ratios $I(E3)/I(E1)$ which range from $8 \cdot 10^4$ to $6 \cdot 10^5$ single particle units.

4. Compilation of Some Properties of the Lowest 3^- States in Even-Even Nuclei

As a result of more refined experimental techniques and increasing interest from the theoretical point of view, the amount of information about the properties of 3^- levels has rapidly increased in the past years. We have made a systematic survey of

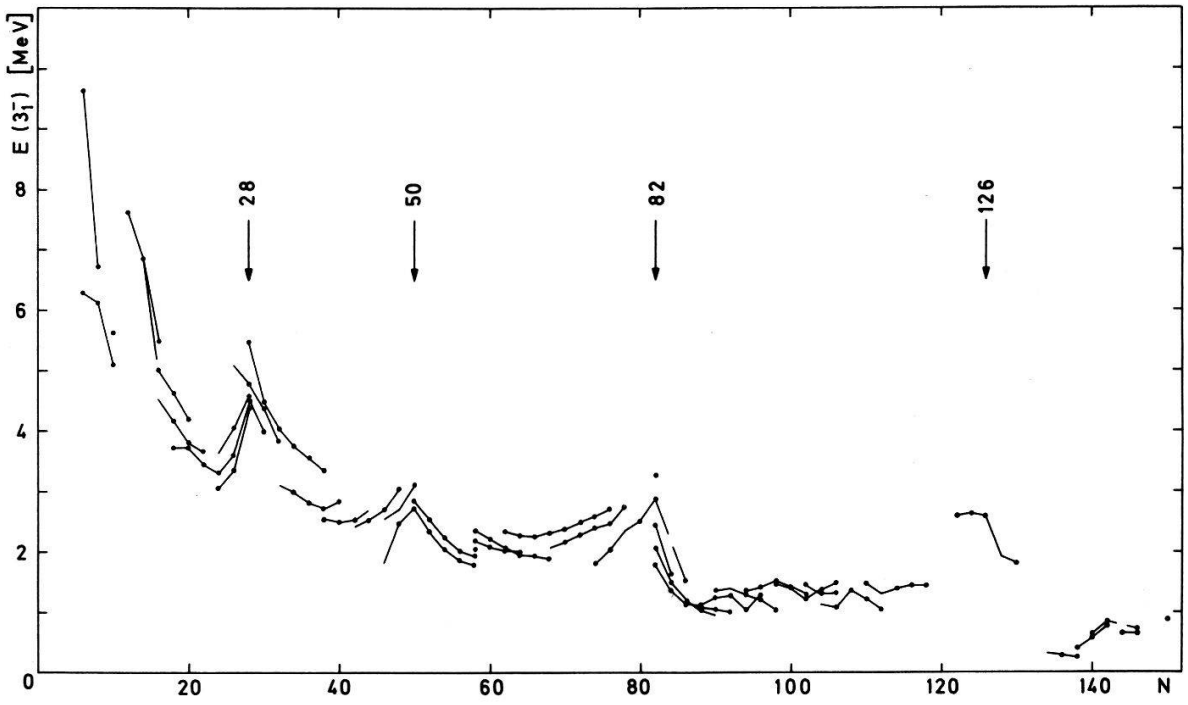

Figure 21
Excitation energies of the lowest 3^- states as a function of neutron number. Isotopes of the same element are connected by solid lines. Where no dot is marked the assignment of 3^- is uncertain. An interruption of a solid line indicates that no 3^- level has been observed.

experimental data [6] and present here some of them in a condensed version. We wish to emphasize that we restricted ourselves to the lowest 3^- level in a nucleus. The data are presented as far as known to the authors up to the end of 1971.

i) Excitation energies. In about 170 nuclei the existence of low-lying 3^- states has been reported most of which have been observed in several kinds of experiments.

Nathan et al. [46] have already pointed out that the energy has the general A-dependence as expected from the liquid drop model, yet the absolute values are only about 40% of the predicted magnitude. Superimposed on this general trend are pronounced shell effects which most distinctly appear in a plot of $E(3_1^-)$ as a function of neutron number (Fig. 21). Relative maxima are observed at the magic numbers 28, 50, 82 and, less pronounced, also around 126. Except in the region of deformed nuclei the relative minima are always at or very near to the middle of these magic numbers.

A similar tendency appears in the Z-dependence (Fig. 22) though somewhat less obviously, probably due to the fact that less nuclei have been investigated in a chain of isotones than in a chain of isotopes. These regularities in $E(3_1^-)$ are very similar to those in $E(2_1^+)$, except that no maximum occurs at either N or Z equal to 20 for the 3_1^- states.

The effect of closed shells on the energy of vibrational states has already been mentioned by Bohr and Mottelson [1], who pointed out that the restoring force parameter C_L is large for these nuclei since they owe their particular stability to the

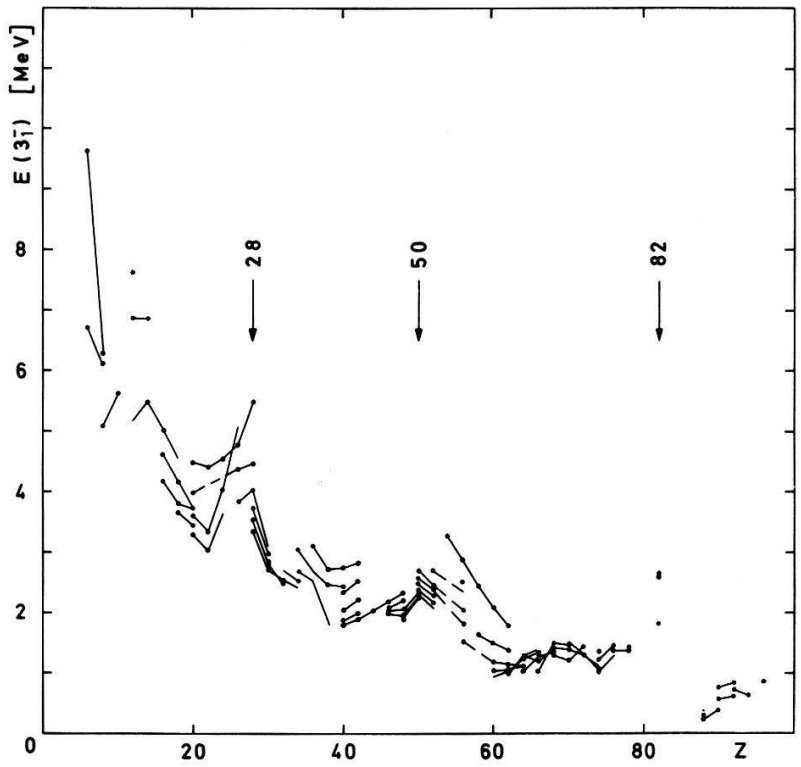

Figure 22
Excitation energies of the lowest 3^- states as a function of proton number. See caption to Figure 21.

spherical form. A large value of C_L results in a high excitation energy E_L because of the well-known relation [1]

$$E_L = \hbar \sqrt{C_L/B_L}.$$

In the regions of deformed nuclei a regular behaviour of $E(3^-)$ is not obvious.

ii) Excitation probabilities. $B(E3)$ values from electromagnetic measurements have been reported for about 70 nuclei and are plotted against neutron number in Figure 23. The data from Hansen and Nathan [21] have not been included in this plot since some authors [47, 48] stated that they are too big, due to a considerable amount of nuclear interaction in the cross-section.

In spite of the apparent similarity between the trends of $E(3_1^-)$ and $E(2_1^+)$ the excitation probability $B(E3)$ varies in a different manner with the neutron number than $B(E2)$ does. The latter shows a distinct shell structure with minima at the magic numbers $N = 28$, 50, 82 and 126 [49], which have been shown by Grodzins [50] to reflect a E^{-1}-dependence of the $B(E2)$ values. A similar dependence of $B(E3)$ does not

exist. Only at $N = 28$ does a minimum occur, but at the other magic numbers, $B(E3)$ is fairly large and even has a maximum at $N = 20$.

Another obvious feature of the $B(E3)$ values is the sharp decrease around $N = 88$ as one goes from spherical to deformed nuclei. In the deformed region the $E3$ strength is often divided among several levels [51] and the lowest 3^- state carries only a fraction of a few single particle units.

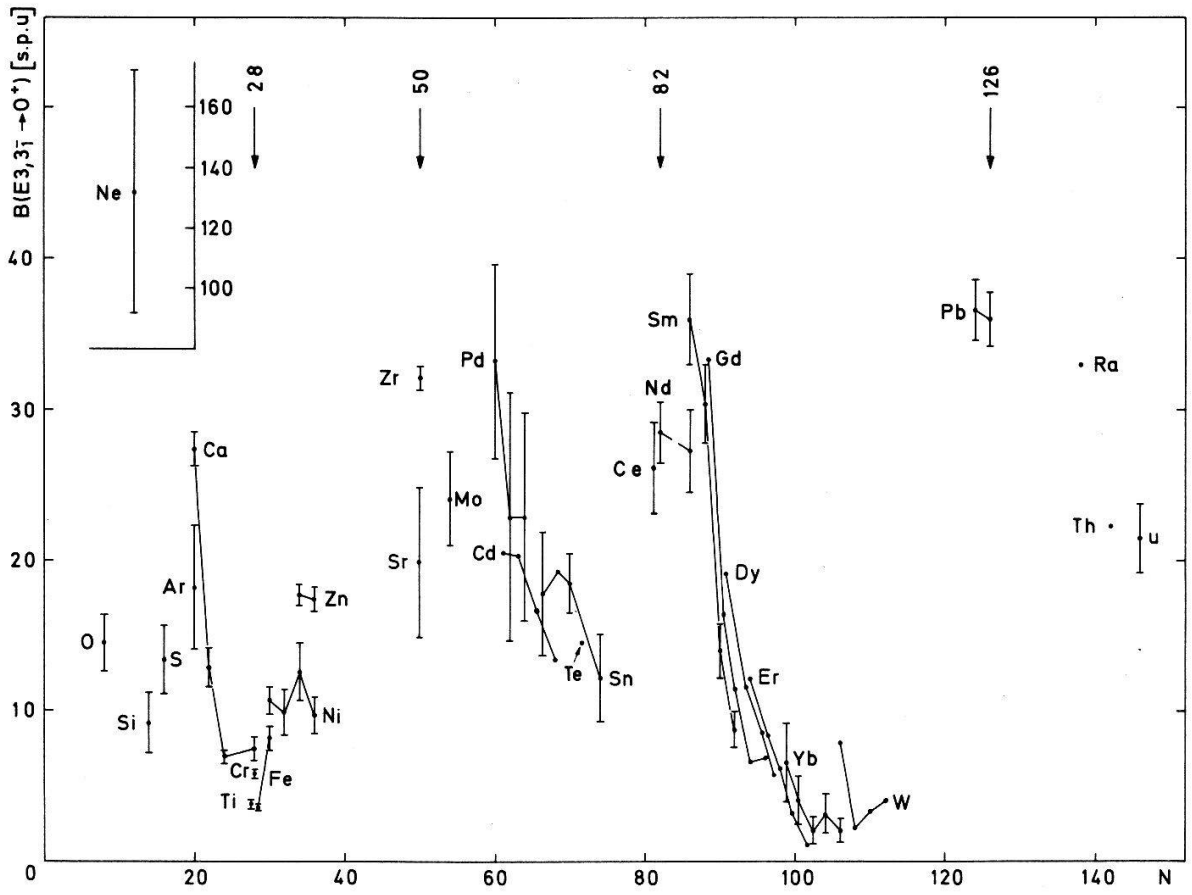

Figure 23

Reduced excitation probabilities $B(E3)$ in single particle units of the lowest 3^- states as a function of neutron number. Isotopes of the same element are connected by solid lines.

iii) *E1 transition probabilities.* As an example for $E1$ transition probabilities of gamma rays depopulating the lowest 3^- states we show in Figure 24 $B(E1, 3_1^- \rightarrow 2_1^+)$. Again we have omitted the data which can be derived from Hansen's $B(E3)$ measurements [21].

The most outstanding feature is the wide spread of data over more than three orders of magnitude. The fastest $3_1^- \rightarrow 2_1^+$ transitions are those in nuclei with the magic neutron numbers 20 and 82, but because only few transition probabilities have yet been measured, it is difficult to decide whether this is a regularity for all magic numbers or not.

From this short survey it is obvious that there exist broad gaps in the experimental information about the properties of low-lying 3^- states in even–even nuclei. The systematics of the excitation energies seem to be well established and need only some completion for the heavy nuclei ($A \gtrsim 190$). For the excitation probabilities the situation is less satisfactory; they have been measured only for about 40% of the

nuclei with known 3^- states and the data are often inaccurate and inconsistent. Very little is yet known about $E1$ transition probabilities. These data are especially useful since they are very sensitive to the details of the wavefunctions of the levels involved and thus provide a valuable check of different nuclear models.

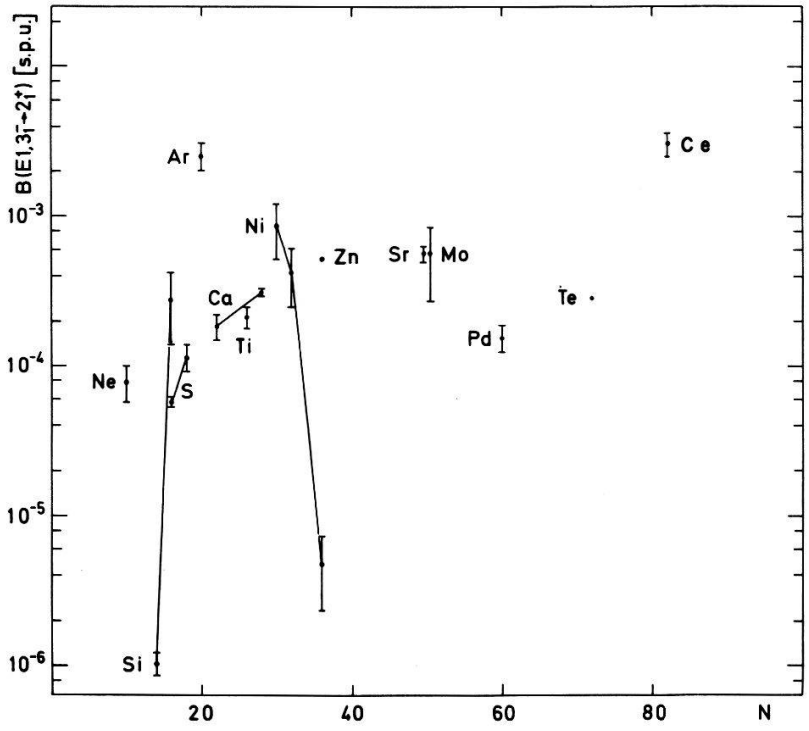

Figure 24
Reduced transition probabilities $B(E1, 3_1^- \rightarrow 2_1^+)$ as a function of neutron number.

Appendix

Peak fitting

Precise gamma ray energy measurements require, apart from other conditions, an accurate determination of the peak positions. If the peak exhibits a pure Gaussian distribution this position is uniquely given by the channel of zero slope. For non-symmetrical distributions the peak position may be defined again as the channel of maximum count rate or alternatively as the centre of the peak area.

The shape of a peak measured by means of a Ge(Li) detector often deviates considerably from a Gaussian distribution due to imperfect crystals (trapping of charge-carriers, edge effects) and (or) imperfect electronics (pile-up). These effects cause a low energy tail of the peak which is superimposed on the original Gaussian distribution and a background which is more intense below the peak than above.

To account for this shape we described a peak by a modified Gaussian which is the sum of a Gaussian $n_1(x)$, a low energy tail $n_2(x)$, a 'step' $n_3(x)$ between the low and the high energy side of the peak and a polynomial $n_4(x)$ (background). We investigated combinations with different $n_2(x)$ and $n_3(x)$ out of which we found the following function giving a good representation of a peak (see Fig. 25):

$$N(x) = \sum_{i=1}^{4} n_i(x)$$

$$n_1(x) = C_1/A \cdot \exp\{-\ln 2 \cdot [(x - C_2)/C_3]^2\}$$

$$n_2(x) = \begin{cases} C_1 \cdot C_4/A\,[(x - C_2)/C_3 + 1]^2 \cdot \exp\{C_5[(x - C_2)/C_3 + 1]\}, & x \leqslant C_2 - C_3 \\ 0, & x \geqslant C_2 - C_3 \end{cases}$$

$$n_3(x) = C_1 \cdot C_6\{0.5 - 1/\pi \cdot \tan^{-1}[(x - C_2)/C_3]\}$$

$$n_4(x) = \sum_{i=7}^{9} C_i \cdot x^{i-7}$$

The normalization constant A is deduced from the condition

$$\int_{-\infty}^{+\infty} [n_1(x) + n_2(x)]\, dx = C_1$$

The peak area was defined as C_1 and the peak position as C_2.

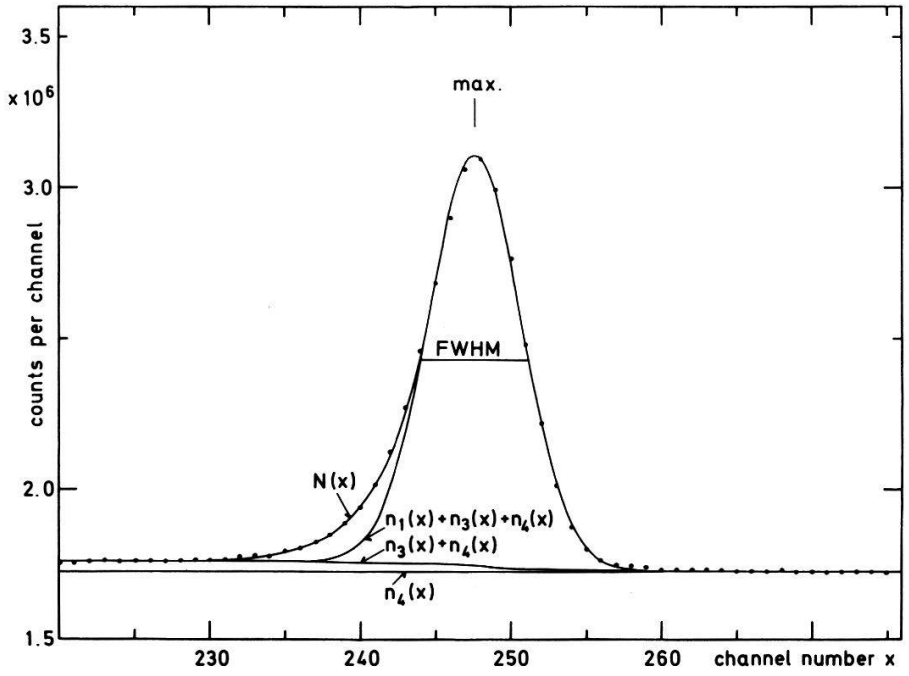

Figure 25
Least squares fit to a typical full-energy peak (432.5 keV transition in the ^{140}La $\rightarrow$ ^{140}Ce decay). The functions $N(x)$ and $n_i(x)$ are defined in the appendix.

The optimal parameters C_i were determined by the least squares method with linearized normal equations as described by Jauneau et al. [52]. The calculations were programmed in FORTRAN and executed on a CDC 1604 A and later on a CDC 6500 in the computing centre of the Swiss Federal Institute of Technology, Zurich. The output of the program supplies the optimal parameters C_i, the error matrix and the value of chi square.

We also used modified versions of this program which execute fits of the function $N(x)$ to the spectrum with one or more of the shape parameters C_3, C_4, C_5 and C_6 maintained at certain values. For peaks covering only a few channels we omitted the low energy tail $[n_2(x) \equiv 0]$ or used pure Gaussian distributions $[n_2(x) = n_3(x) \equiv 0]$.

Acknowledgments

I am grateful to Professor Dr. J. P. Blaser for the continued support of this work. I express my great appreciation to Professor Dr. H. J. Leisi for his constant interest, many helpful comments and encouraging discussions. It is a pleasure to thank Messrs. Dr. H. Dirren, Dr. F. N. Gygax, Th. von Ledebur, Dr. R. Lombard, M. Roth and D. Taqqu for their assistance to the experiments and numerous stimulating discussions. Mr. W. Schoeps helped greatly with the electronic instrumentation and gave much extra time, for which I am very grateful. Many thanks are due to Mr. H. Haug for the mechanical construction. I thank Mr. J. D. Sykes for carefully reading the manuscript.

REFERENCES

[1] A. Bohr and B. R. Mottelson, Mat. Fys. Medd. Dan. Vid. Selsk. *27* (16) (1953).
[2] K. Alder, A. Bohr, T. Huus, B. Mottelson and A. Winther, Rev. Mod. Phys. *28*, 432 (1956).
[3] S. A. Moszkowski, in *Alpha-, Beta- and Gamma-Ray Spectroscopy*, Vol. 2, edited by K. Siegbahn (North-Holland Publ. Co., Amsterdam 1965), p. 863.
[4] W. C. Barber, Ann. Rev. Nucl. Sci. *12*, 1 (1962).
[5] A. Z. Schwarzschild and E. K. Warburton, Ann. Rev. Nucl. Sci. *18*, 265 (1968).
[6] F. C. Roehmer, in preparation.
[7] C. M. Lederer, J. M. Hollander and I. Perlman, *Tables of Isotopes*, 6th ed. (Wiley, New York 1967).
[8] B. L. Robinson, Phys. Rev. *140*, B1529 (1965).
[9] W. R. Phillips, Nucl. Phys. *60*, 544 (1964).
[10] R. G. Allas, L. Meyer-Schützmeister and D. von Ehrenstein, Nucl. Phys. *61*, 289 (1965).
[11] Th. von Ledebur and F. C. Roehmer, Helv. Phys. Acta *40*, 340 (1967); *41*, 1289 (1968).
[12] R. Hess, F. C. Roehmer, F. Gassmann and Th. von Ledebur, Nucl. Phys. *A137*, 157 (1969).
[13] G. Murray, R. L. Graham and J. S. Geiger, Nucl. Phys. *63*, 353 (1965).
[14] R. L. Robinson, P. H. Stelson, F. K. McGowan, J. L. C. Ford, Jr. and W. T. Milner, Nucl. Phys. *74*, 281 (1965).
[15] L. Jarczyk, J. Lang, R. Müller and W. Wölfli, Helv. Phys. Acta *34*, 483 (1961).
[16] J. van Klinken, F. Pleiter and H. T. Dijkstra, Nucl. Phys. *A112*, 372 (1968).
[17] F. Erné, W. A. M. Veltman and J. A. J. M. Wintermans, Nucl. Phys. *88*, 1 (1966).
[18] K. Lieb, H. Röpke, H. Grawe, H. J. Brundiers and O. Klepper, Nucl. Phys. *A108*, 233 (1968).
[19] G. A. P. Engelbertink, H. Lindeman and M. J. N. Jacobs, Nucl. Phys. *A107*, 305 (1968).
[20] G. A. P. Engelbertink and G. van Middelkoop, Nucl. Phys. *A138*, 588 (1969).
[21] O. Hansen and O. Nathan, Nucl. Phys. *42*, 197 (1963).
[22] H. W. Baer, J. J. Reidy and M. L. Wiedenbeck, Nucl. Phys. *A113*, 33 (1968).
[23] F. C. Roehmer and H. J. Leisi, Helv. Phys. Acta *42*, 912 (1969).
[24] M. Roth and F. C. Roehmer, Helv. Phys. Acta *43*, 419 (1970).
[25] D. C. Camp and A. L. Van Lehn, Nucl. Instr. and Meth. *76*, 192 (1969); *87*, 147 (1970).
[26] M. J. L. Yates, in *Alpha-, Beta- and Gamma-Ray Spectroscopy*, Vol. 2, edited by K. Siegbahn (North-Holland Publ. Co., Amsterdam 1965), appendix 9.
[27] H. Appel, in Landolt-Börnstein, *Numerical Data and Functional Relationships in Science and Technology*, New Series, Group I, Vol. 3, edited by K.-H. Hellwege (Springer-Verlag, Berlin–Heidelberg—New York 1968).
[28] L. A. Sliv and I. M. Band, in *Alpha-, Beta- and Gamma-Ray Spectroscopy*, Vol. 2, edited by K. Siegbahn (North-Holland Publ. Co., Amsterdam 1965), appendix 5.
[29] M. E. Wiedenbeck and D. E. Raeside, Nucl. Phys. *A176*, 381 (1971).
[30] L. C. Biedenharn and M. E. Rose, Rev. Mod. Phys. *25*, 729 (1953).
[31] W. W. Black and A. C. G. Mitchell, Phys. Rev. *132*, 1193 (1963).
[32] H. H. Bolotin, C. H. Pruett, P. L. Roggenkamp and R. G. Wilkinson, Phys. Rev. *99*, 62 (1955).

[33] W. H. KELLEY and M. L. WIEDENBECK, Phys. Rev. *102*, 1130 (1956).
[34] R. M. LEVY and D. A. SHIRLEY, Phys. Lett. *3*, 46 (1962).
[35] N. KAPLAN, S. OFER and B. ROSNER, Phys. Lett. *3*, 391 (1963).
[36] H. J. KÖRNER, E. GERDAU, C. GUNTHER, K. AUERBACH, G. MIELKEN, G. STRUBE and E. BODENSTEDT, Z. Physik *173*, 203 (1963).
[37] G. R. BISHOP and J. P. PEREZ Y JORBA, Phys. Rev. *98*, 89 (1955).
[38] R. C. BANNERMAN, G. W. LEWIS and S. C. CURRAN, Phil. Mag. *42*, 1097 (1951).
[39] S. E. KARLSSON, B. SVAHN, H. PETTERSSON and G. MALMSTEN, Nucl. Phys. *A100*, 113 (1967).
[40] F. C. ROEHMER, to be published in Helv. Phys. Acta.
[41] R. PITTHAN, Z. Naturforsch. *25a*, 1358 (1970).
[42] G. ARDISSON and C. MARSOL, J. Phys. Soc. Japan *30*, 1194 (1971).
[43] M. A. LUDINGTON, J. J. Reidy, M. L. WIEDENBECK, D. J. MCMILLAN, J. H. HAMILTON and J. J. PINAJIAN, Nucl. Phys. *A119*, 398 (1968).
[44] R. E. MCADAMS and O. H. OTTESON, Z. Physik, *250*, 359 (1972).
[45] E. P. GRIGORIEV, K. Y. GROMOV, ZH. T. ZHELEV, T. A. ISLAMOV, V. G. KALINNIKOV, U. K. NAZAROV and S. S. SABIROV, Izv. Akad. Nauk SSSR (ser. fiz.) *33*, 635 (1969).
[46] O. NATHAN and S. G. NILSSON, in *Alpha-, Beta- and Gamma-Ray Spectroscopy*, Vol. 1, edited by K. SIEGBAHN (North-Holland Publ. Co., Amsterdam 1965), p. 601.
[47] G. BRUGE, J. C. FAIVRE, H. FARAGGI and A. BUSSIERE, Nucl. Phys. *A146*, 597 (1970).
[48] C. LECLERCQ-WILLAIN, J. de Phys. *32*, 833 (1971).
[49] P. H. STELSON and L. GRODZINS, Nucl. Data *1*, 21 (1965).
[50] L. GRODZINS, Phys. Lett. *2*, 88 (1962).
[51] B. ELBEK, T. GROTDAL, K. NYBØ, P. O. TJØM and E. VEJE, Proc. Int. Conf. on nuclear structure, Tokyo 1967; J. Phys. Soc. Japan Suppl. *24*, 180 (1968).
[52] L. JAUNEAU and D. MORELLET, Notions de statistique et applications, in *Proceedings of the 1964 Easter School for Physicists*, Vol. 1 (CERN 64-13).